ISTANBUL TECHNICAL UNIVERSITY ★ GRADUATE SCHOOL

COATING OF SILVER DOPED TITANIUM BY BIODEGRADABLE PCL TO DELAY ANTIBACTERIAL SILVER RELEASE IN DENTAL IMPLANTS

M.Sc. THESIS

Gizem Özge KAYAN

Department of Metallurgical and Materials Engineering

Materials Engineering Programme

FEBRUARY 2021

ISTANBUL TECHNICAL UNIVERSITY ★ GRADUATE SCHOOL

COATING OF SILVER DOPED TITANIUM BY BIODEGRADABLE PCL TO DELAY ANTIBACTERIAL SILVER RELEASE IN DENTAL IMPLANTS

M.Sc. THESIS

Gizem Özge KAYAN
(506181412)

Department of Metallurgical and Materials Engineering

Materials Engineering Programme

Thesis Advisor: Assoc. Prof. Dr. M. Reza NOFAR

FEBRUARY 2021

ISTANBUL TEKNİK ÜNİVERSİTESİ ★LİSANSÜSTÜ EĞİTİM ENSTİTÜSÜ

DİŞ İMPLANTLARINDAKİ ANTİBAKTERİYEL GÜMÜŞ SALINIMINI GECİKTİRMEK İÇİN GÜMÜŞ KATKILI TİTANYUMUN BİYOÇÖZÜNÜR PCL İLE KAPLANMASI

YÜKSEK LİSANS TEZİ

Gizem Özge KAYAN
(506181412)

Metalurji ve Malzeme Mühendisliği Anabilim Dalı

Malzeme Mühendisliği Programı

Tez Danışmanı: Doç.Dr. M. Reza NOFAR

ŞUBAT 2021

Gizem Özge Kayan, a M.Sc. student of İTU Graduate School of Science Engineering and Technology student ID 506181412, successfully defended the thesis entitled "COATING OF SILVER DOPED TITANIUM BY BIODEGRADABLE PCL TO DELAY ANTIBACTERIAL SILVER RELEASE IN DENTAL IMPLANTS", which she prepared after fulfilling the requirements specified in the associated legislations, before the jury whose signatures are below.

Thesis Advisor : **Assoc. Prof. Dr. M. Reza NOFAR** ....
İstanbul Technical University

Jury Members : **Prof. Dr. Hüseyin ÇİMENOĞLU** ....
Istanbul Technical University

Prof. Dr. Erdem ATAR ....
Gebze Technical University

Date of Submission : 22 December 2020
Date of Defense : 10 February 2021

To my family

FOREWORD

Throughout the writing of this thesis I have received a great deal of support and assistance. I wish to thank all the people whose assistance was a milestone in the completion of this study.

I would first like to thank my supervisor, Assoc. Prof. Dr. M. Reza NOFAR, whose expertise was invaluable, his insightful feedback sharpened my thinking and brought my work to a higher level. I would like to express my sincere appreciation to Prof. Hüseyin ÇIMENOĞLU for his support and for his guidance to further my research.

I would like to acknowledge the financial supports from Istanbul Technical University Scientific Research Project (ITU-BAP) – Master Thesis Project with the project number of 42388.

I would like to acknowledge Prof. Asgar KAYAN for valuable contribution in running characterizations in his laboratory, specifically for providing FTIR and GPC equipment. I also would like to thank Prof. Lütfi ÖVEÇOĞLU for the opportunity I was given in order to get EDS analysis.

In addition, I would like to thank Doğukan ÇETINER, Faiz MUAFFEL and Mertcan KABA for the help they provided for MAO, SEM and XRD experiments. Also, I would like express my sincere gratitude to Yonca ALKAN for her encouragement and helping during the FTIR and AAS characterizations. Many thanks to all technical and administrative staff of ITU Faculty of Chemical and Metallurgical Engineering for their kind cooperation during this work.

From the bottom of my heart I would like to say big thank you to Burcu ÖZDEMIR, Doğan ARSLAN and Göksel HIZLI for the support and motivation they provided throughout my thesis. Last but not least, I would like to thank my family for their patience and encouragement.

February 2021

Gizem Özge KAYAN
(Metallurgical and Material Engineer)

TABLE OF CONTENTS

Page

ABBREVIATIONS

AAS	: Atomic Absorpion Spectroscopy
AgNPs	: Silver nanoparticles
ASTM	: American Society for Testing and Materials
$CHCl_3$	: Chloroform
EDS	: Energy-dispersive X-ray spectroscopy
FTIR	: Fourier Infrared Sppectroscopy
GPa	: Gigapascal
GPC	: Gel Permation Chromatography
HA	: Hydroxyapatite
MAO	: Micro-arc oxidation
MPa	: Megapascal
PBS	: Phosphate buffer saline
PCL	: Polycaprolacton
PLA	: Polylactide
ROP	: Ring Opening Polymerization
SBF	: Stimulated body fluid
SEM	: Scanning electron microscope
$SnCl_2$	: Tin(II) Chloride
THF	: Tetrahydrofuran
Ti	: Titanium
TiO_2	: Titanium oxide
XRD	: X-ray scattering

SYMBOLS

ρ	**:** Density
g	**:** Gravity
h	**:** Thickness of coating
mV	**:** Milivolt
M_w	**:** Molecular weight
Tg	**:** Glass transition temperature
Tm	**:** Melting temperature
U	**:** Withdrawn speed
γ_{LV}	**:** Surface tension
η	**:** Viscosity of liquid

LIST OF TABLES

Page

LIST OF FIGURES

Page

COATING OF SILVER DOPED TITANIUM BY BIODEGRADABLE PCL TO DELAY ANTIBACTERIAL SILVER RELEASE IN DENTAL IMPLANTS

SUMMARY

Since biodegradable polymers are obtained from natural sources and are sustainable, their use is increasing day by day. When biopolymers degrade, they turn into harmless and non-toxic products, which makes them widespread in many areas, especially in biomedical use. Polycaprolacton (PCL) is a biocompatible and biodegradable aliphatic linear polyester obtained by ring-opening polymerization of ε-caprolactone monomer. Thanks to its low glass transition temperature (-60 ° C) and its remarkable toughness value, PCL has superior properties compared to other biopolymers with its processability. In addition, its low rate of degradation depending on field of usage, its ability to dissolve in many solvents and its permeability to drug release are among the other advantages of PCL.

The aim of this thesis is to delay the release of silver by coating biodegradable PCL on the titanium oxide layer containing silver in dental implants. Cr-Co alloys, stainless steel and titanium are widely used as implant materials. Special consideration was paid to chose a base metal which is biocompatible, has a close Young module value with the bone and has a high corrosion resistance. The proximity of the Young's modulus values of the bone and implant material to each other minimizes the shielding effect that causes abrasion and loosening of the implant material. Considering these parameters, titanium has been determined as the most suitable base material. The next step is to obtain a porous titanium oxide layer on titanium metal by micro-arc oxidation (MAO) method. Micro-arc oxidation technique can be defined as creating an arc on the anode by applying negative voltage to the anode sample used as the base immersed in the electrolyte solution and positive voltage to the cathode, and then oxide coating of the surface of the base material. A porous structure, which is important for controlled drug release, was obtained by MAO. In addition, with this method, the corrosion resistance of the base and the adhesion between the coating and the base were increased. After that, in order to delay the silver release, the PCL solution was prepared to coat the base. Due to the slow degradation of PCL, $SnCl_2$, which acts as a catalyst, was added at the rates of 5, 20, 40, 60 and 80% of PCL. The optimum rate for minimum toxicity and high degradation, two the most important parameters, was determined as 5 % and the base was coated with the prepared solution by using dipping method. The prepared samples were kept in SBF (simulated body fluid) at 37 °C, normal body temperature, for 1-4 weeks and characterization was performed every week. As a result of the characterization performed by optical microscope, it was observed that MAO significantly increased adhesion.

Another result obtained from optical microscopy analysis is that starting from the first week to the fourth week, formation of amorphous biomimetic HA increased significantly on the examined surfaces. By the fourth week, the maximum amount of amorphous biomimetic HA was observed and this was a positive factor for the

formation of bone between the bone and the implant. This study is also an in vitro characterization method. Moreover, a very bright image of the biomimetic HA caused the optical microscope figure to be unclear. In SEM analysis, it was seen that the Ti bases had a porous structure at the end of the silver-free MAO method, but the silver-doped sample formed dendritic structures. The structures formed on the surface were determined by EDS and XRD analysis. During the preliminary study, GPC analysis were performed to observe the degradation of PCL, and as a result of these analysis, it was found that the degradation percentage of PCL pellets in SBF was 1.5% on the 7th day and 22.5% on the 28th day. After this determination, PCL solution containing 5% $SnCl_2$ of PCL was prepared in chloroform and then this solution was dipped as a thin film on the Ti-base.

According to the GPC and FTIR results, which support the results of this experiment, the PCL and ε-caprolactone in the SBF fluid of the 4th week are more distinct than the 1st week. In addition, it was found from GPC analysis that the coating was thinner than the pellet, and therefore degraded more. Carbonate apatite peaks were found in the analysis of the SBF solution made with FTIR, which indicates that the implant is biocompatible according to the BS ISO 23317: 2014 standard. The amount of silver release was measured with the help of the last characterization, Atomic Absorption Spectroscopy (AAS) analysis. In order to measure the effectiveness of PCL, AAS analysis of both polymers coated and uncoated samples were performed under the same conditions. At the end of the measurements, it was observed that the maximum amount the release of uncoated samples was on the first day and it decreased day by day and by the 6th day it reached the values below the reading limit of the device. Therefore, measurement could not be made after the 6th day. Looking at the coated samples, a steady increase in silver release was observed from the 1st week to the 4th week. As a result, all characterization results showed that PCL containing $SnCl_2$ released silver within the targeted time.

DİŞ İMPLANTLARINDAKİ ANTİBAKTERİYEL GÜMÜŞ SALINIMINI GECİKTİRMEK İÇİN GÜMÜŞ KATKILI TİTANYUMUN BİYOÇÖZÜNÜR PCL İLE KAPLANMASI

ÖZET

Biyobozunur polimerlerin doğal kaynaklardan elde edilmesi ve sürdürebilir olması nedeniyle kullanımı gün geçtikçe artmaktadır. Biyopolimerler bozunduğunda zararlı veya toksik olmayan ürünlere dönüşürler ki bu özellikleri birçok alanda özellikle de biyomedikal kullanımında yaygınlaşmasını sağlamaktadır. Polikaprolakton (PCL), ε-kaprolakton monomerinin halka açılması polimerizasyonu yoluyla elde edilen biyo-uyumlu ve biyobozunur alifatik lineer bir polyesterdir. Polikaprolakton yarı kristalin bir polimerdir. Buna ilave olarak, PCL düşük camsı geçiş sıcaklığı (-60 °C) ve kayda değer tokluk değeri sayesindeki işlenebilirliği ile diğer biyopolimerlerle kıyaslandığında üstün özelliklere sahiptir. Ayrıca, amaca yönelik düşük bozunma hızı, birçok çözücü içinde çözünebilme özelliği ve ilaç salınımındaki geçirgenliği polikaprolaktonun diğer avantajları arasında yer alır.

Bu tez kapsamındaki amaç, diş implantı olarak saf titanyum altlığı üzerine yapılan mikro ark yöntemiyle gümüş ihtiva eden titanyum oksit tabakasının üzerine biyobozunur PCL kaplanması ile gümüş salınımının geciktirilmesidir. Antibakteriyel bir özellik istenmesinin sebebi, bakterilerin sebep olduğu biofilm oluşumunu engellemektir. Biofilm oluşumu sonucunda enfeksiyon ve iltihaplanma gibi istenmeyen durumlarla karşılaşılır ve bu da implant malzemesinin etkinliğini azaltır. Dahası, iyileşme süreci de uzar. Bütün bu negatif etkileri minimize etmek amacıyla antibakteriyel ajan katkılandırılması gerekir. Daha etkili bir implant elde edebilmek için antibakteriyel etki süresinin uzatılması istendi. Bu amaçla, antibakteriyel ajan ile katkılandırılan implant üzerine bir kaplama yapıldı. Etkili bir implant için önemli bir diğer parametre ise ideal bir altlık malzemesi seçilmesidir. İmplant malzemesi olarak CrCo alaşımları, paslanmaz çelik ve titanyum yaygın olarak kullanılmaktadır. Altlık olarak seçilecek metalin biyo-uyumlu olmasına, kemik ile arasındaki Young’s Modulünün birbirlerine yakın olmasına ve korozyon direncinin yüksek olmasına dikkat edilmiştir. Kemik ile implant malzemesinin Young’s modulü değerlerinin birbirlerine yakın olması, aşınma, kırılma ve implant malzemesinin gevşemesine neden olan gerilme kalkanı (shield stress) etkisini minimuma indirger. Ayrıca, implant olarak seçilecek altlık malzemesinin düşük yoğunluğa sahip bir metal olması istenir. Bunun sebebi, implant olarak kullanıldığı zaman vücutta ilave bir ağırlık oluşturmaktan kaçınılmasıdır. Bu parametreler göz önüne alındığında titanyum en uygun altlık malzemesi olarak belirlenmiştir. Sonraki aşama, titanyum metali üzerine mikro-ark oksidasyon (MAO) yöntemi ile porlu bir yapıya sahip titanyumoksit tabakası elde edilmesidir. Mikro ark oksidasyon tekniği, elektrolit çözelti içerisine daldırılmış altlık olarak kullanılan anot numuneye negatif voltaj, katoda ise pozitif voltaj uygulanmasıyla anot üzerinde ark oluşturulması ve altlık malzemesinin yüzeyinin oksit kaplanması olarak tanımlanabilir. SEM sonuçlarına bakıldığında, mikro ark oksidasyon yöntemi ile kontrollü ilaç salınımı için önemli olan porlu bir yapı elde edildiği görüldü. Ayrıca bu yöntemin etkisini incelemek amacıyla MAO

uygulanmış ve uygulanmamış saf Ti üzerine polikaprolakton kaplaması yapıldı. Bu numuneler yapay vücut sıvısı içerisinde 1 hafta bekletildi. Bir hafta sonunda optik mikroskop ile yapılan karakterizasyon sonucunda, MAO uygulanmayan saf titanyumun yüzeyine PCL kaplamasının yapışmadığı ve yüzeyden ayrıldığı görüldü. Mikro ark oksidasyon yöntemi, altlığın korozyon direncinin ve kaplama ile altlık arasındaki yapışmanın artmasıyla sonuçlandı. Mikro ark oksidasyon yöntemi ile doplanan gümüşün yüzeyde dentritik yapılar oluşmasına sebep olduğu görüldü. Ardından, gümüş salınımının geciktirilmesi amacıyla altlığın üzerine kaplamak üzere polikaprolakton çözeltisi hazırlandı. Ancak, PCL'nin bozunma hızının düşük olması gümüş salınımının istenilen sürede gerçekleşmesine engeldir. Bu kapsamda, PCL'nin yavaş bozunumunu hızlandırmak amacıyla katalizör görevi gören %5, 20, 40, 60 ve 80 oranlarında $SnCl_2$ eklendi. Kalay klorürün PCL üzerindeki katalizör etkinliğinin ölçülmesi için PCL pelletleri üzerinde ön bir çalışma yapıldı. PCL pelletleri üzerinde yapılan ön çalışmada kalay klorürün etkili olduğu görüldü. Ancak, kalayın insan vücudu üzerinde olumsuz etkileri olduğu bilinmektedir. Önemli parametrelerden olan minimum toksisite ve yüksek bozunum hızının en uygun değer olduğu oran %5 olarak belirlendi ve gümüş katkılı mikro ark uygulanmış altlık, hazırlanan çözelti ile daldırma yoluyla kaplandı. Kaplanan numuneler çözücünün uzaklaştırılması amacıyla 40 °C' de 12 saat boyunca etüvde tutuldu. Ardından, hazırlanan numuneler SBF (yapay vücut sıvısı) içerisinde vücut sıcaklığı olan 37 °C'de 1-4 hafta bekletildi ve her hafta karakterizasyon yapıldı. Optik mikroskop analizi sonucunda, birinci haftadan başlayarak dördüncü haftaya kadar incelenen yüzeylerde oluşan amorf biyomimetik hidroksi apatitin (HA) belirgin bir şekilde arttığı görüldü. Dördüncü haftaya gelindiğinde, biyomimetik HA'nın miktarının maksimum olduğu ve bunun kemik ile implant arasındaki kemik oluşu için pozitif bir etken olduğu görülmüştür. Yapılan bu çalışma aynı zamanda biyouyumluluğu gösteren bir in vitro karakterizasyon yöntemidir. EDS ve XRD analizleri ile yüzeyde oluşan yapılar belirlendi. PCL kaplanmamış numunelerin XRD ve EDS sonuçlarına bakıldığında, gümüş doplanan ve doplanmayan MAO uygulanmış Ti numunelerinin ortak özellikleri bulundu. Her ikisinde de titanium, anataz, rutil ve kalsiyum titanat pikleri görüldü. Buna ek olarak, gümüş doplanan numunede ekstra pikler görüldü ve yapılan literatür sonucunda bu piklerin Ag_2O' ya ait olduğu belirlendi. Ön çalışma sırasında PCL'nin bozunumunu gözlemlemek için GPC analizleri yapıldı ve bu analizler sonucunda SBF içerisindeki PCL pelletlerinin 7. günde %1,5 olan bozunum yüzdesinin 28. günde %22,5 olduğu saptandı. Bu tespitten sonra, PCL' nin %5'i kadar $SnCl_2$ içeren PCL çözeltisi kloroform içerisinde hazırlandı ve ardından bu çözelti Ti-altlığı üzerine ince film olarak daldırma yöntemiyle kaplandı. Kaplanan numunelerin, SBF' in içerisine daldırıldıktan 1-3 hafta sonra XRD analizleri yapıldı. Bu karakterizasyon sonucunda, hidroksi apatit piklerine rastlandı ve gümüş salınımına bağlı olarak Ag_2O piklerinde azalma görüldü. Literatürde Ag_2O'nun sadece (111) pikinin kararlı olmasının sebebi, gümüş ile oksijenin bağ uzunluğunun kısa olmasına bağlı olarak kovalent bağ etkileşiminin fazla olmasına bağlanmıştır. Kovalent bağ o düzlemin hidrofob olması ile sonuçlanır ve bu da SBF içerisinde kararlı olmasını sağlar.

Bu deney çıktılarını destekler nitelikte alınan GPC ve FTIR sonuçlarına göre, 4. haftanın SBF sıvısının içerisindeki PCL ve ε-kaprolakton 1. haftaya göre daha belirgindir. Buna ek olarak, GPC analizi yapılan kaplamanın pellete oranla daha ince olması nedeniyle daha fazla bozunmaya uğradığı tespit edildi. Kalay klorür içeren PCL filminin ilk hafta sonunda % 42.63, 4 hafta sonunda ise % 57.27 bozunduğu görüldü. Optik sonuçlarını destekler nitelikte olan FTIR ile yapılan SBF çözeltisinin analizinde karbonat apatit piklerine rastlandı ki bu BS ISO 23317:2014 standardına göre implantın biyouyumlu olduğunu gösterir. Yapılan bir diğer analiz olan pH değerlerinin değişimleri incelendiğinde ilk gün 7.4 olan SBF solüsyonunun pH değerinin, PCL kaplanmamış numunede 28 gün sonunda 7.99 değerine yükseldiği belirlendi. Bu yükselişin sebebi, kuvvetli bir baz olan hidroksi apatit oluşumuna bağlandı. PCL kaplanmış numunelerin 28 gün sonundaki pH değeri 7.89 olarak bulundu. Numunelerin kaplanmasıyla pH değerinin 7.99 iken 7.89 değerine düşmesi, polikaprolaktonun bozuması sonucu oluşan 6- hidroksi kaproik asit oluşumu olarak belirtildi. Son olarak, atomik absorpsiyon spektroskopisi (AAS) analizi ile gümüş salınım miktarı ölçüldü. PCL'nin etkinliğini ölçmek için aynı standartlarda hem polimer kaplanmış hem de kaplanmamış numunelerin atomik absorpsiyon spektroskopisi analizi yapıldı. Yapılan ölçümler sonucunda, kaplanmamış olan numunelerin 1. gün maksimum olmak koşuluyla gün geçtikçe salınım miktarının azaldığı ve 6. gün itibariyle cihazın ölçüm limitinin dışına çıktığı gözlendi. Kaplanan numunelere bakıldığında ise 1. haftadan 4. haftaya gümüş salınımında düzenli bir artış gözlendi. Bunun nedeni, polikaprolakton filminin bozunmasıyla gümüşün salınımının gerçekleşmesidir. PCL kaplanmayan numunelerin 6 günde salınımını yaptığı gümüş miktarı %100 alındığında, PCL kaplanan numunelerin 28 gün sonundaki gümüş salınımı %85 olarak bulundu. Sonuç olarak bu tez kapsamında yapılan bütün karakterizasyon sonuçları $SnCl_2$ içeren PCL'nin hedeflenmiş süre içerisinde gümüş salınımını gerçekleştirdiğini gösterdi.

1. INTRODUCTION

Controlled drug release has been one of the concerns in medical area because of the importance of adjusting the healing time in biomedical applications. Knowing the release rate and time of the drugs or antibacterial agents determine the treatment. Initial burst release is the one of the unwanted phenomena which hinders sustainable release. There are some methods in order to prevent the initial burst such as coating with polymers and encapsulation [1]. Coating with biodegradable polymers is used more commonly due to its superior properties [2-3]. There has been an increase in usage of biodegradable polymers to decrease the concerns about the conventional petroleum-based polymers' negative impacts on the environment. Biodegradable polymers also known as biopolymers are obtained from renewable materials or all-natural plants or living micro-organisms. The structure of these polymers makes them readily break down easily into non-toxic and eco-friendly final products by natural micro-organisms [4]. Polycaprolacton (PCL) is a biodegradable and biocompatible polymer that is produced from ε-caprolacton by ring opening polymerization (ROP) [5,6].

PCL is a semi-crystalline polymer at room temperature and human body temperatures, as well. PCL has low Tg (glass transition temperature (-60 °C)) which increases the process-ability, melting temperature (58-63 °C) and significant toughness [7,8]. In addition, solubility in wide range of solvents mostly in organics and permeability of many drugs are some advantages of PCL. Moreover, having a slow degradation rate is another benefit of PCL for long-term implants [9-11]. Thus, PCL has a lot of remarkable properties such as being eco-friendly, biocompatible and having unique mechanical and chemical features which make a good candidate for many applications, especially in biomedical field.

The aim of this thesis is to dope an antibacterial silver into Ti dental implant to prevent biofilm formation caused by bacterias. Also, to provide delay antibacterial silver release by coating by biodegradable PCL. As a base metal, titanium is chosen instead of other implant materials such as CrCo alloys, stainless steels and zinc alloys in order to reduce corrosion, shield stress and inflammation [12]. Moreover, titanium is a light metal which is a significant parameter for implant materials. Titanium has the closest Young's modulus to the bone compared to other materials which is an essential parameter to prevent the shield stress. The result of Young modulus difference between the bone and material can be defined as stress-shielding phenomenon. Wear and loosening of the implant, fracturing again and non-healing of a bone can be the reasons of the mismatching between the Young modulus [13,14].

After that, micro-arc oxidation (MAO) process is applied on the pure titanium. MAO is a process in which used high voltage plasma in order to assist anodic oxidation process [15]. MAO results in highly porous oxide ceramic structure on the surface of metal. To have a regular spherical porous structure, voltage, time and electrolytes of MAO were altered.

Silver is used as an antibacterial agent in micro arc oxidation electrolyte in the form of silver acetate. The reason of applying silver instead of copper, zinc and bismuth is that silver has a higher antibacterial activity against bacteria and release rate [16].

The last step of experiment part is coating the silver doped MAO coated pure titanium with biodegradable PCL by using dip coating method. As it was said before, the purpose is to delay release of silver ions coated with PCL. Since the degradation of polycaprolactone takes 2-3 years, $SnCl_2$ was used as a degradation catalyst to accelerate this process. PCL was used in different wt % to evaluate the effect of viscosity on the thickness of film. As the thickness of the film is an important parameter in degradation, the best coating solution was achieved by 5% wt. PCL (95% wt. $CHCl_3$) due to its ideal viscosity to have homogeneous solution and coating thickness. A primerely experiment was done with PCL pellets and tin chloride. Different amounts of tin chloride were used to investigate the catalyst activity on PCL pellets. Considering the toxicity and degradation activity of tin, $SnCl_2$ was used as 5% of the amount of PCL used in the actual experiment. GPC and FTIR analysis were used to characterize the degradation of PCL. To determine the controlled delayed silver release and the degradation of PCL in body, simulated body fluid (SBF) was used. The temperature of SBF was 37 ºC which is normal body temperature and pH value was 7.4. The samples are soaked in SBF for 1 to 4 weeks.

When the optical microscope, Fourier transform spectroscopy, gel permeation chromatography, and atomic absorption spectroscopy characterization results were evaluated, it was determined that the amorphous biomimetic HA was formed and degradation products of PCL were seen. Also, it was observed that PCL gradually degraded within the targeted time (up to the 4^{th} week). It was also measured that silver release increased in parallel with the degradation of polycaprolactone. Within the scope of this thesis, it was found that delayed silver release can be achived by coating of silver doped titanium by biodegradeble polymers and using effective catalysts.

2. LITERATURE REVIEW

2.1 Controlled Antibacterial Agent Release

Drugs are either natural or synthetic chemicals which cure, prevent or reduce signs of diagnoses. They are ingested into living organisms by various kinds of ways such as by implants, medicines and encapsulation applications [1]. A drug delivery can be identified as a system which promotes getting better treatments of therapeutic materials into the human body by changing the period, rate and location of drugs [17]. Drug delivery systems have several benefits such as having more accurate results in local area, reducing toxicity and being economical for both patients and providers. Although drug delivery system has a lot of benefits, releasing the drugs at the initial stage is a negative side of this system. Therefore, to overcome this problem controlled drug delivery has been investigated. Controlled drug release is a phenomenon about inhibiting the initial burst release which hinders a sustainable drug delivery [2]. Improvement in convenience, having preferable patient compliances, stabilization of medical situations due to uniformity in drug amounts and reduction in drug utilization and accumulations can be listed as positive consequences of controlled drug release [18]. Coating with biodegradable polymeric materials and encapsulation are the methods for controlling the rate and time of drugs.

There are four general mechanisms of drug delivery systems which are controlled by diffusion, chemistry, solvents and adjustable systems. Diffusion controlled drug delivery which is used in membrane applications. It is designed as either a membrane or matrix. Diffusion of drug determines the rate of drug release. Polymeric membrane covers all the drug part which is the part dissolves in membrane at first and after that penetrates into polymer molecules through outside of membrane. Although matrix system is easier to produce, the initial burst of drug is much higher. The important part of this mechanism is that having a polymeric material which is wanted to dissolved in preferred time range. As the polymer dissolves the length of molecule becomes shorter and diffusion gets higher and better [19].

Chemical controlled mechanisms are based on three stages: gradual biodegradation of drug loaded polymer, degradation of drug bonds attached to polymer and diffusion of drug from membranes. The degradation of polymers can be hydrolytic or enzymatic and in both ways it results in drug release. The rate of drug release depends on the bond rapture between the drug and polymer [20].

Solvent controlled system is the third mechanism which affect the drug release. When the suitable solvent contacts the polymer, the chains of the polymer get loosened. This stage occurs when the glass transition temperature of polymer is below than the process temperature. Loosening and swelling determines the rate of drug release in this situation.

The last one is an adjustable mechanism which means changing the temperature, pH and UV lights according to used materials and systems [19].

2.1.1 Antibacterial agents for drug release

There is an alternative approach which uses using antibacterial or antimicrobial metals rather than utilizing medicines/drugs. Silver, gold, platinum, copper and zinc are the most commonly used metal ions in order to prevent bacterial adhesion on the implant. Selection of the right metal includes some features like being non-toxic, non-allergic to mammalian cells and being effective to bacteria. Sometimes, double metal coatings are applied to have desired properties. For example, Hwang-Sog Ryu et al. [21] investigated the influence of adding platinum into silver for orthodontic appliances to see whether the platinum increases the mechanical characteristics or not. Stainless steel was used as a base material and antibacterial coating was applied by vapor deposition technique. The results showed that adding a small amount of platinum in silver increase the mechanical properties but antimicrobial effect on Streptococcus mutans and Aggregatibacter actinomycetemcomitans did not change remarkably and the vapor deposition method was not an effective way.

Malachova et al. [22] studied the influence of montmorillonite in antibacterial and antifungal specialties by using silver, copper and zinc. The results showed that when montmorillonite was used instead of free metal ions, the difference of antibacterial effiency between these two was not different from each other (Figure 2.1).

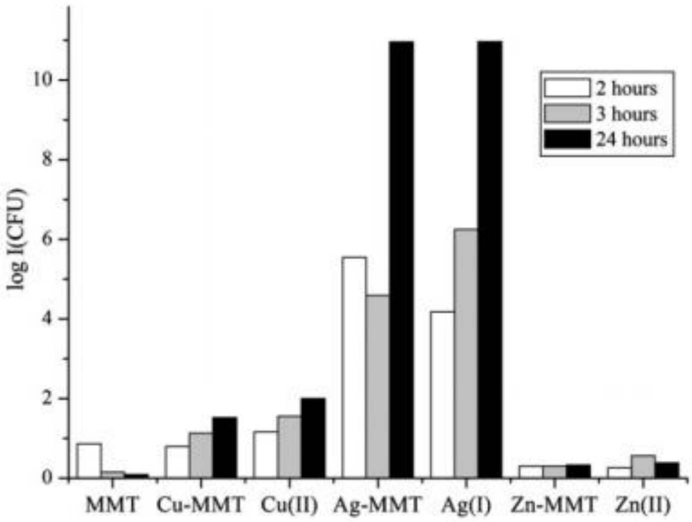

Figure 2.1: Antibacterial efficiency of copper, silver and zinc which expressed as logarithms of I versus time [22].

On the other hand, the influence of different kinds of antibacterial metal ions on various types of bacteria differs. For example, silver showed the highest antibacterial property on E. coli bacteria and copper and zinc followed the order, respectively. Pycnoporus cinnabarinus bacteria formation was least for zinc, and then copper and silver. Pleurotus ostreatus decreased in the order copper, zinc and silver [22]. Moreover, another study about silver, gold and platinum indicated that silver had the best antibacterial effect on gram negative bacteria compared to both grams positive one and the other metal ions [23]. Also, there are some specific locations that the effects of certain elements are considerably good. For instance, bismuth is commonly used in gastricus problems such as gastritis or ulcers. Marshall et al. [24] stated that the healing process could be improved by adding colloidal bismuth in drugs for gastric mucosa. To conclude, some elements can be used as antibacterial and antimicrobial agents in particular applications. Among these elements, silver is one of the most common one because of its utilization in different areas in human body and preventing bacterial colonization against most bacteria. Also, it has minimum toxicity to mammalian creatures since it has superior toxicity to bacteria.

2.1.1.1 Silver

Silver is the one of the most common and effective metal ion as it was mentioned above. The studies about silver have been increased since 1800's. It can be used in the form of silver nitrate and silver acetate as the source of silver ion or silver nano particles. Antibacterial characteristic is desired in implant materials generally since the healing time is long and the formation of bacteria film is possible. Dental implants are the applications in which preventing the formation of bacteria film is essential. Moreover, using silver instead of antibiotics is because the penetration of antibiotics in biofilm which is generated by bacteria is very hard [25,26]. The saliva environment and eaten food lead up to the formation of bacteria. To evaluate the formation of Staphylococcus aureus, Zhang et al. [27] studied silver doped micro arc oxidation coated pure titanium. In vitro experiment resulted in decreasing the formation of S. aureus bacteria when the amount of silver was increased as shown in the Figure 2.2.

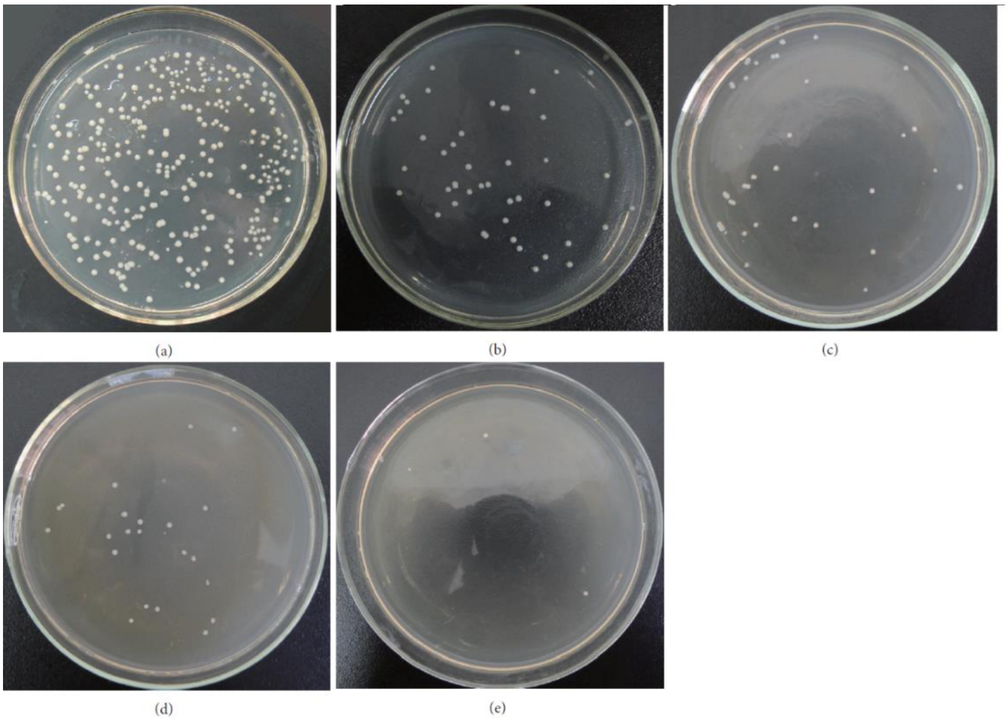

Figure 2.2: Images of in antibacterial vitro test against *S. aureus*: (a) control specimen Ti-MAO, (b) Ti-MAO-Ag1.0, (c) Ti-MAO-Ag5.0, (d) Ti-MAO-Ag10.0, and (e) Ti-MAO-Ag20.0.

The other study the one Wang et al. [28] showed the efficiency of silver on E. coli bacteria. They said that the effectiveness of silver up to 5% is very dominant but after increasing the concentration of silver to higher than 5%, the differences could not be seen clearly. Another output of from this study is that antibacterial experiment can be done by UV irradiation.

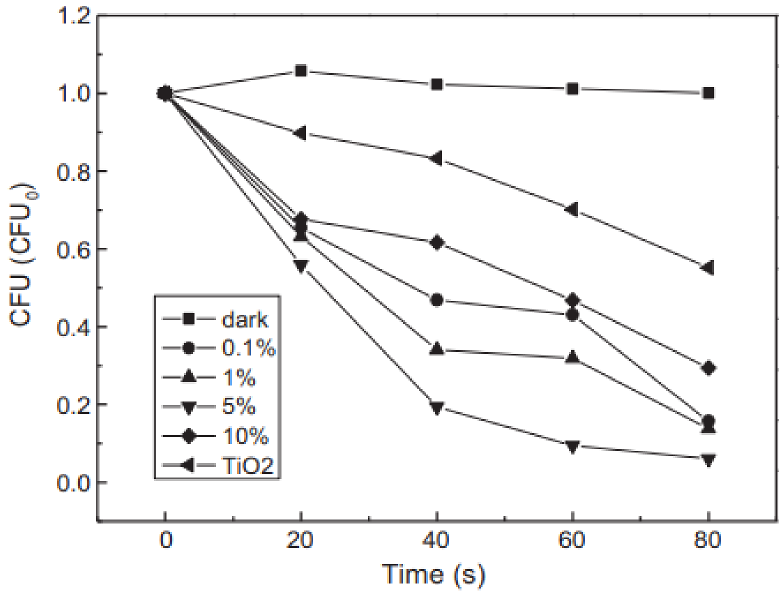

Figure 2.3: The inactivation efficiency of E. coli bacteria on various amount of silver (0–10%) doped TiO_2 thin films under UV irradiation and in the dark [28].

It can be emphasized that silver as an ion plays a crucial role in antibacterial applications and its influences on various type of bacteria have been explained in the litearure, especially on the basis of dental implant applications.

2.1.1.1 Antibacterial mechanism of silver

Antibacterial silver has been studied for a long time to prevent the biofilm formation. Biofilm formations causes to imflammatory, infections and insufficient cell attachments. In order to have an effective implant, antibacterial agents like silver should be used. However, the act of antibacterial mechanism is not very clear. There are some theories about this phenomena [29-31]. According to Yun'an Qing et al. [25] there are two kinetics of antibacterial properties which are accepted. It is concluded that silver nanoparticles are attached to the bacterial cell wall and as a result leak into it. This situation causes physical changes in the bacterial membrane. For example, deterioration of membrane causes to cell membrane leakage and to death of bacteria (Figure 2.3). Furthermore, cellular membrane of bacteria is known to be negatively charged because of the existence of phosphate, carboxyl, and amino groups. Since silver has positive charge, the electrostatic attraction between the cellular membrane and silver is irresistible. From this moment, silver can also penetrate into bacterial cell [32, 33].

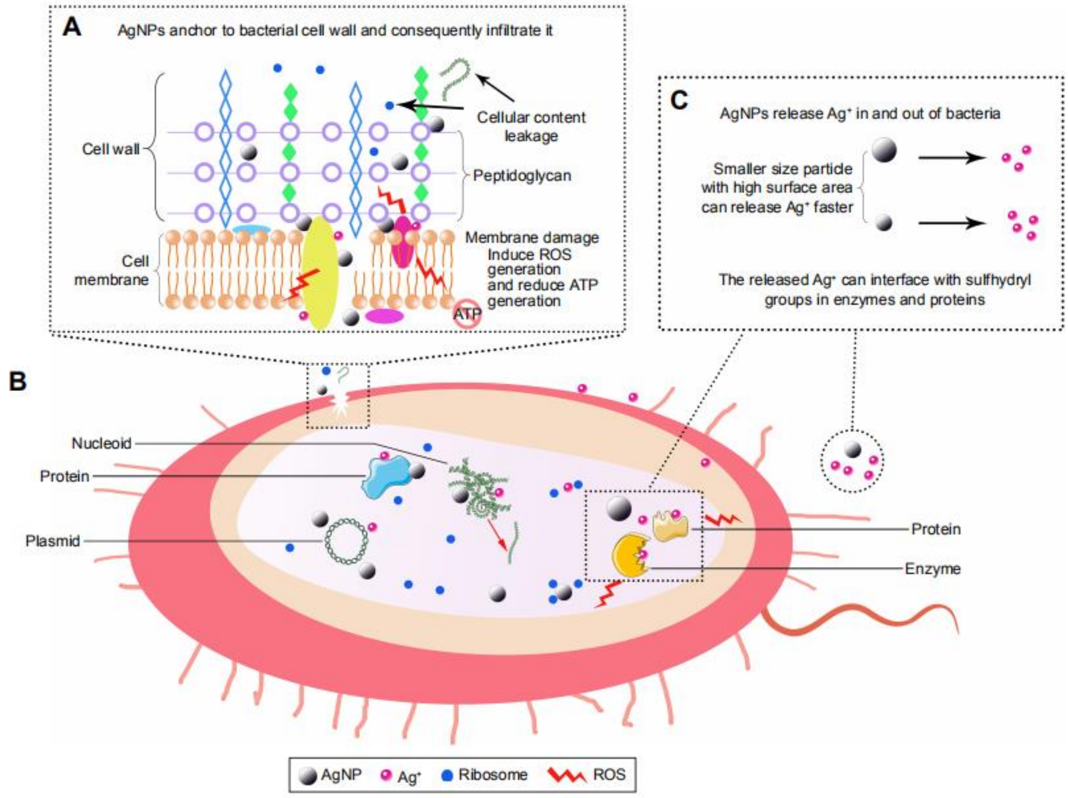

Figure 2.4: Antibacterial kinetics of silver nanoparticles (AgNPs) [25].

After silver nanoparticles are absorbed by the cell, the interaction between proteins, lipids, DNA and silver can be observed which results in bacterial function disorder and death. When silver interacts with ribosomes, the situation can end up with denaturation and inhibition of translation and protein synthesis (B section of Figure). In addition, as it can be seen from the Figure 2.4, there are some reactive oxygen species (ROP) like hydrogen peroxides, super oxides and radicals and these reactive oxygen materials can be formed by silver particles. Finally, the kinetics of the antibacterial feature of Ag^+ is showed in Figure 1C in which its interface with sulfhydryl groups in enzymes and proteins can be seen. Ag^+ can attach to proteins that exist in the cell membrane to produce stable bonds and it is concluded with protein deactivation. Last but not least, ability to form complex and interaction with nucleic acids and nucleosides of Ag^+ has been detected [34].

2.2 Biopolymers

In recent years, biopolymers have been highly investigated according to their sustainability and their benefits to environment compared to traditional petroleum-based polymers. Biopolymers can be defined as polymers produced from living organisms, microbial sources, natural materials or biodegradable synthetic monomers [4]. Figure 2.5 shows that when a polymer is classified, there are four parameters which are being bio-based or not and biodegradable or non-biodegradable. For example, PCL is one of the most known one in fossil-based and biodegradable polymer whereas the PLA and PBS are both bio-based and biodegradable polymers.

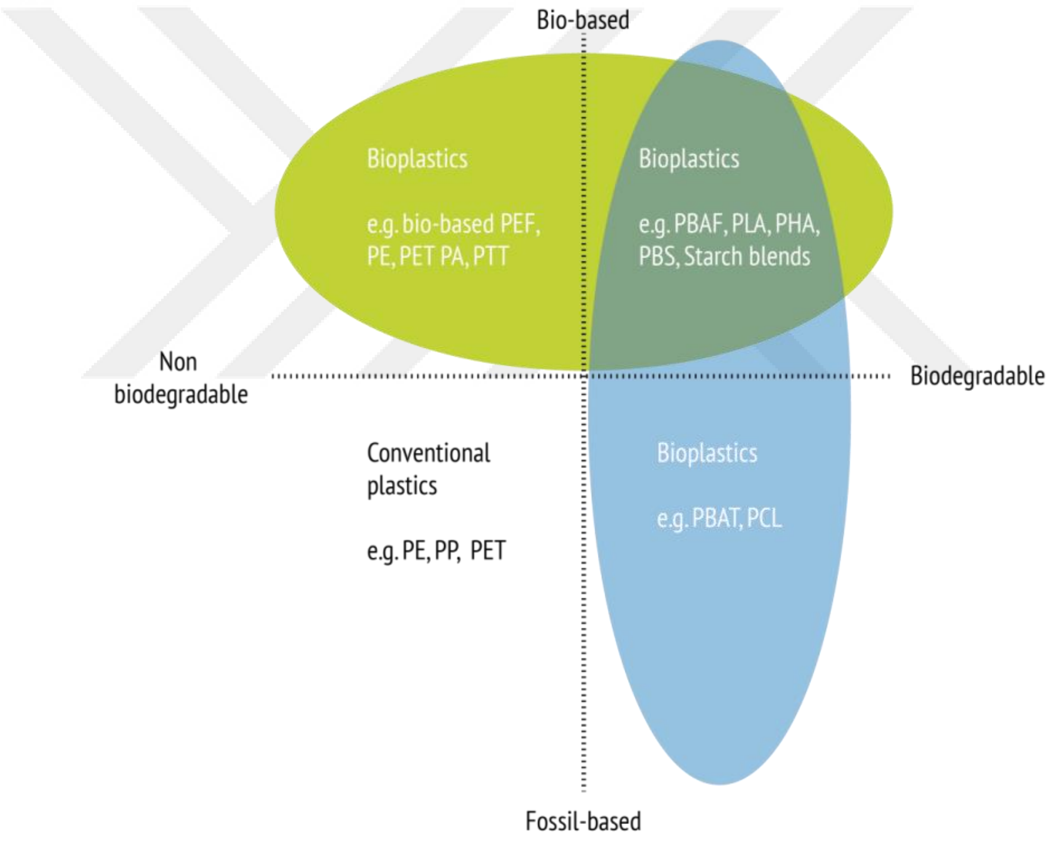

Figure 2.5: Classification of biopolymers [35].

Also, biopolymers are a branch of biodegradable polymers which means that they can be biodegraded [9,36]. When degradation of biopolymers takes place, the final products or by-products are generally non-toxic and have no side effects. This could be the major factor of the increase in studies about biopolymers.

2.2.1 Degradation process in biodegradable polymers

The usage of biodegradable polymers has been increasing over the past years because of the benefits they offer. Beside its advantages while using it, effects of degradation products cannot be underestimated. Hence, when these polymers are used, the requirements of applications should match the properties of polymer. Also, after the degradation takes place, the evaluation of mechanical and chemical properties, alteration in micro and macro scale can be seen. Therefore, the degradation kinetics, by and final products of polymers should be known to select the right material for particular field especially in tissue engineering, drug release and cell growth. To understand and predict the degradation behavior of biodegradable polymers, three main processes are given.

- Chemical and Enzymatic Oxidation
- Enzyme-Catalyzed Hydrolysis
- Non-Enzymatic Hydrolysis

Chemical and enzymatic oxidation can happen when the biodegradable polymer subjected into human body or tissues. This process is called chemical oxidation because of presence of oxidation products which can be seen during inflammatory because of surrounding with highly reactive oxygen materials (superoxide, hydrogen peroxide etc.) when the foreign material is exposed. These chemical reactions can be improved by changing the temperatures, pH values, pressure or time which are also affect the act of enzyme kinetics [37]. After a certain time, these reactive materials begin to degrade the polymer chains and molecules.

Catalyzes are the acceleration materials that are used in chemical reactions. When a catalyze is generated from biological materials, it is called enzymes. Acceleration is not only the mission of enzymes, in fact for human body they are crucial. If the sufficient amount of enzyme cannot be found, then most of the metabolism functions would be impracticable. Hydrolytic enzymes can exist in oral, gastrointestinal tract and human body plasma. A degradation controlled by an enzyme takes place in four levels. Enzymes from solution penetrate into the surface of substrate and then, enzyme-substrate complex is formed. The third stage takes place when the hydrolysis reaction is accelerated by an enzyme catalysis. The final stage is the migration of soluble materials after degradation process through the solution. Enzyme catalyzed hydrolysis can be influenced by molecular weight, degree of crystallinity, pH, temperature, and medium [38]. Presence of enzymes in degradation process can change the degradation rates compared to absence of them. That can be the reason of not having an accurate and same result in vivo and in vitro experiments. In vitro tests are done because of their easy, simple and nature-friendly characteristics. Moreover, the results can be foreseeable by using in vitro test for medical applications. Simulated body fluid (SBF), and phosphate buffer saline (PBS) solution are used in vitro tests to mimic the body plasma like in vivo test. However, these solutions do not contain enzymes compared to human body plasma. For this reason, when the SBF or PBS are used in vitro tests, solely normal hydrolysis is expected. For instance, Azevedo et al. [38] confirmed that lipase which is an enzyme for hydrolysis of the ester bonds of PCL in vivo experiment can accelerate the degradation rate. Although SBF, is used for in vitro experiments, has not any enzymes to accelerate the reaction that results in slower degradation rate [39].

When water molecules meet with polymeric material, the hydrolytic degradation can be observed. Scission of chemical bonds in the polymer backbone causes this type of degradation and because of cleavage of bonds, polymer transforms into oligomer and monomer in the last stage. Acids, bases and salts can act as a catalyze which can accelerate the hydrolysis reactions. This reaction also depends on the nature of material which can be either hydrophobic or hydrophilic. Hydrolysis mechanism consist of the following stages. First, the water attacks the polymer and then, polymer absorbs the water and swells. The degradation starts from the outside and proceed through the inside of the polymer with an order. First, hydrolysable bonds cleavage in hydrophilic and hydrophobic, respectively. Then, no hydrolysable bonds cleavage with this order: hydrophilic and hydrophobic. It is known that all biodegradable polymers have hydrolysable bonds like esters, glycosides and anhydrides.

2.2.1.1 Hydrolytic degradation

Photo, thermal, chemical and mechanical mechanisms are the possible different types of mechanism when a polymer degrades. The degradation mechanism can be one or combination of them but in many cases, combination is seen. If a polymer degrades by scission of chains and results in reduction in mechanical properties because of an aqueous media, it can be defined as hydrolytic degradation. This mechanism can be accelerated by changing the pH by adding acids or bases and enzymes as catalysts. The rate of degradation can be determined by various parameters such as length of polymer chain, crystallinity, porosity and pore size of matrix, molecular weight of polymer, size figure and the morphology of matrix and experiment conditions [9, 40, 41].

Polyesters, polyorthoesters and polyanhydrides undergo a hydrolysis reaction because of having ester bonds in their structure. Even though the type of degradation mechanism is known, where the degradation takes place is an unknown. To have information whether it is a surface or bulk degradation, diffusion and hydrolysis kinetics should be known.

The degradation starts from the surface, if the rate of hydrolysis is higher than diffusion of environment into the bulk material. Working with hydrophobic polymers, having high Tg, highly crystalline structure and chemical structures of polymers can be the reasons of lower diffusion rate. The penetrated water or environment in the bulk can be found by diffusion coefficient and solubility of studied polymer.

Bulk degradation or erosion happens when the diffusion of water or environment into polymer is greater than hydrolysis reaction. Presence of acidic or basic oligomers and monomers as degradation products will increase the rate of diffusion. Bulk degradation is a mechanism where the degradation is homogenous all over the thickness [42-44].

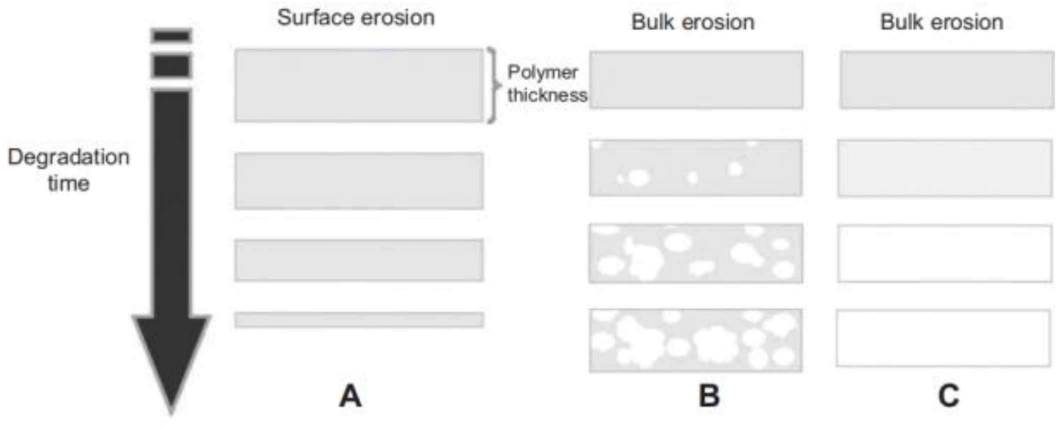

Figure 2.6: Schematic representation of surface and bulk erosion [44].

As it is seen from the Figure 2.6, there are two types of bulk erosion which are with and without auto catalyzed. Fig (B) shows bulk degradation mechanism with auto catalyzed which causes the generation of porous structure because of loss of eroded material. When a pore achieves a critical size because of mechanical or swelling stresses, there can be loss of mechanical features of material. Moreover, diffusion of water or environment through a polymer is faster than oligomers with acidic end groups. Thus, the deposition of acidic end groups results in heterogeneous erosion. Fortunately, this phenomenon can be preventable by adjusting the thickness of polymer so that the diffusion of degraded materials diffuses swiftly.

On the one hand, there are some certain polymers which are eroded via bulk degradation mechanism. Polylactic acid, poly (glycolic acid) and poly(ε-caprolacton) are the examples for polyesters. It can be said that the presence of ester bonds in the polymer triggers the bulk degradation mechanism. Moreover, the number of the ester bonds are important parameter in degradation mechanisms as well. On the other hand, some of the polyanhydrides and polycarbonates are prone surface degradation.

Even though the degradation mechanism can be predictable according to chosen polymer, type of degradation can be influenced by crucial factors which are the critical value of thickness, pseudo first order rate of hydrolysis and diffusion coefficient. The Figure 2.7 shows the relation between the equations and degradation mechanisms. So, if the critical thickness is higher than coating thickness of polymer, bulk degradation controls the mechanism. In bulk degradation mechanism, the loss of mass becomes after the loss of molecular weight and mechanical features like strength. M_w and durability of material reduce from the initial stage of experiment. Appearance of polymer does not change until the polymer degrades at a certain critical value. The reason of remaining still of mechanical properties at bulk erosion is that reducing in molecular weight cannot influence the mechanical characteristics of the polymer since physical cross-linkages because of entanglements and crystal phases which form the architecture of the material. Furthermore, the decrease in mass happens when the degradation products are formed and increased as a soluble material due to presence of carboxylic acid end groups. These carboxylic acid end groups increase the rate of hydrolysis because of having acidic pH values. So, as the carboxylic acid end groups increase the loss of mass also increases. To sum up, molecular weight reduces until at a critical point and after that loss in mass occurs.

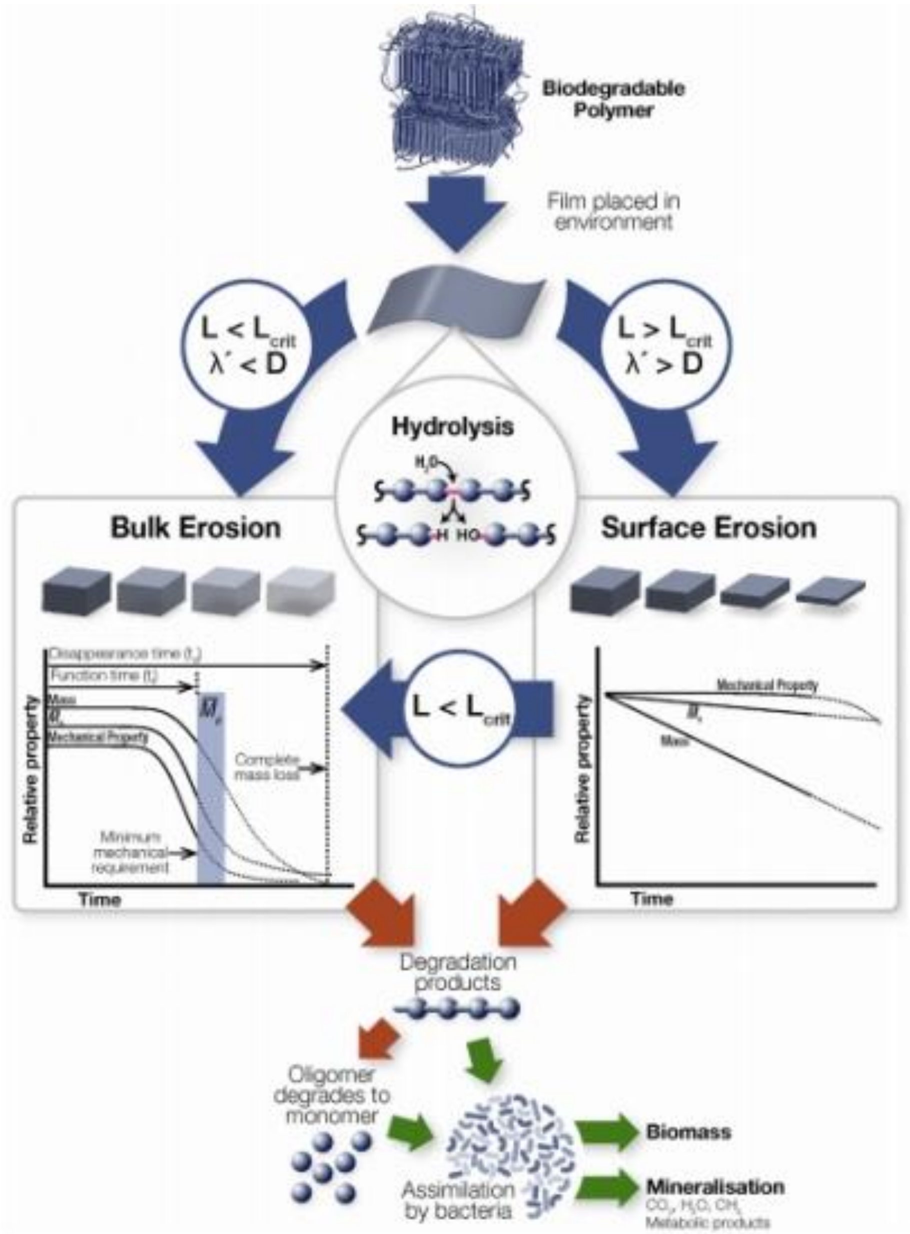

Figure 2.7: Mechanism of surface and bulk degradation [9].

On the other part, the mechanism for surface degradation is completely opposite. This type of degradation happens when hydrolysis of polymer is faster then diffusion of environment. In surface degradation mechanism, first of all loss of mass is observed and the reduction of mass is proportional to polymer's surface area. Since surface degradation starts from the surface, degradation can be noticed from outside. In addition, size and shape of polymer change by the time. Finally, difference in molecular weight can be seen after a critical point.

2.2.2 Polycaprolactone (PCL)

As it was mentioned before, the usage of biopolymers has been increasing due to their superior properties compared to traditional petroleum-based polymers. So, utilization of biopolymers has been long recognized as a significant phenomenon in the field ranging from food packaging to tissue engineering. When the classification of biodegradable polymers is observed, four different branches are observed such as micro- organisms, biotechnology and petrochemical products. Considering the Figure 2.8, it is seen that the classification of polymers is based on whether their monomers are of synthetic or natural origin.

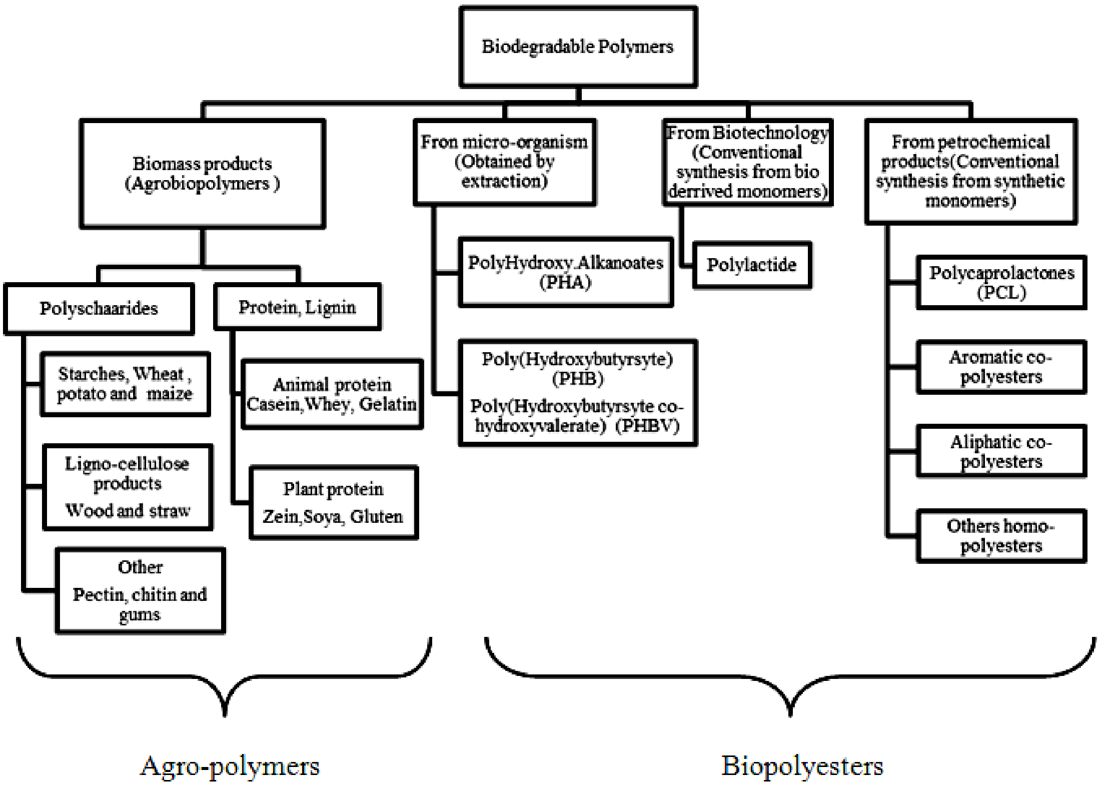

Figure 2.8: Classification of biodegradable polymers [46].

As it can be seen from the figure above, polycaprolactone is a fossil based polymer which is obtained by conventional synthesis from synthetic monomers. Also, PCL is linear aliphatic polyester and produced by ring opening polymerization (ROP) process of ε-caprolactone. ROP process is initiated by anionic, radical or coordination polymerization mechanisms [47, 48]. Coordination polymerization mechanism of PCL is given in Figure 2.9.

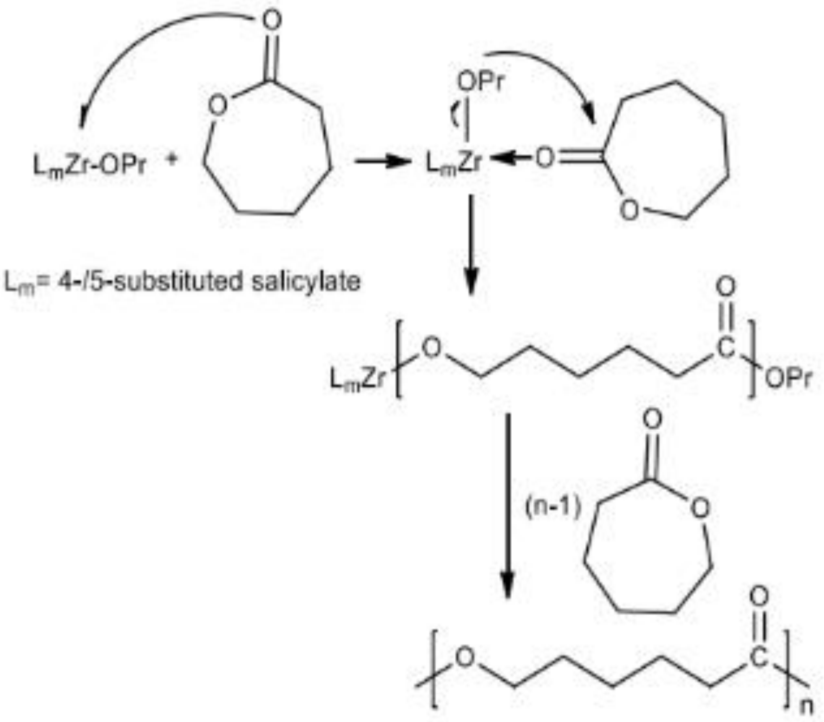

Figure 2.9: Coordination-insertion mechanism for ROP of ε-caprolactone [47].

Polycaprolactone is a semi-crystalline polymer at room and human body temperatures. PCL has low Tg (-60 °C) which increases the process-ability, Tm (58-63 °C) and significant toughness [5-8]. In addition, solubility in wide range of solvents and permeability of many drugs are some advantages of PCL. Thus, PCL has a lot of remarkable properties such as being eco-friendly, biocompatible and having unique mechanical and chemical features which result in being a good candidate for wide range of applications.

2.2.2.1 Soluability of PCL

PCL has variety of usage areas due to its blend compatibility and solubility in different materials and solvents. It is reported that solubility of PCL in organic solvents are generally higher when it is compared to other biopolymers. This leads PCL to be a coating material by Sol-Gel and dissolution processes. Table 2.1 shows the solubility of PCL in different type of solvents in formula and degree of solubility. Higher solubility is desired for many applications to have a homogenous and regular coating. Although, it is said that it has a good solubility characteristic, its dissolution in water and alcohols are very low compared to others.

Table 2.1: Solubility of PCL in different chemicals [49].

Chemicals	Formula	Solubility
Benzene	C_6H_6	High
Carbon tetrachloride	CCl_4	High
Chloroform	$CHCl_3$	High
Cyclohexanone	$C_6H_{10}O$	High
Tolune	C_7H_8	High
2-nitropropane	$C_3H_7NO_2$	High
Acetone	C_3H_6O	Low
Acetonitrile	C_2H_3N	Low
2-butanone	$CH_3COCH_2CH_3$	Low
Dimethylformamide	C_3H_7NO	Low
Ethyl acetate	$C_4H_8O_2$	Low
Water	H_2O	Insoluble
Ethyl alcohol	C_2H_5OH	Insoluble
Diethyl ether	$(C_2H_5)_2O$	Insoluble

Choosing the solvent is not the only way but it is the best way to have a preferable solution. As in tailoring the controlled drug release rate, temperature, and time affect the dissolution of polymers in solvents. Solvents should be chosen based on their melting and evaporation temperatures and the utilization fields. When it will be used in especially in biological areas, non-toxic, non-allergic and not harmful chemicals should be selected. Unfortunately, there are toxic and harmful but also very effective chemicals in the table. At this point, the evaporation temperature dominates the process since the polymer which dissolves in the solvent is known. For instance, chloroform is not a healthy material for biomedical applications however it is commonly used because of having its low evaporation temperature (61 °C) compared to degradation temperature of PCL.

2.2.2.2 Dissolution of PCL

The influence of polymer dissolution plays a key role in industrial fields like tissue engineering, drug delivery and membrane systems. Knowing the dissolution mechanism of a polymer allows to improve the quality of processes or designs by changing the type of polymer, solvent and time. In addition, the reason of using the minimum amount of polymer is to prevent the waste of material. For this reason, dissolution kinetics has been investigated for last decades. Dissolution of polymers is determined by two parameters such as disentanglement of chains and chain diffusion.

One of which is disentanglement of chains and the other one takes place through the boundary layer by chains diffusion. The ways of dissolutions of non-polymeric and polymeric materials are completely different from each other. Non-polymeric one's result at once whereas the polymers go through two processes which are solvent diffusion and chain disentanglement. Diffusion takes place when the thermodynamically compatible solvent and an amorphous polymer meet and after that, polymer becomes a gel-like form as the time passes.

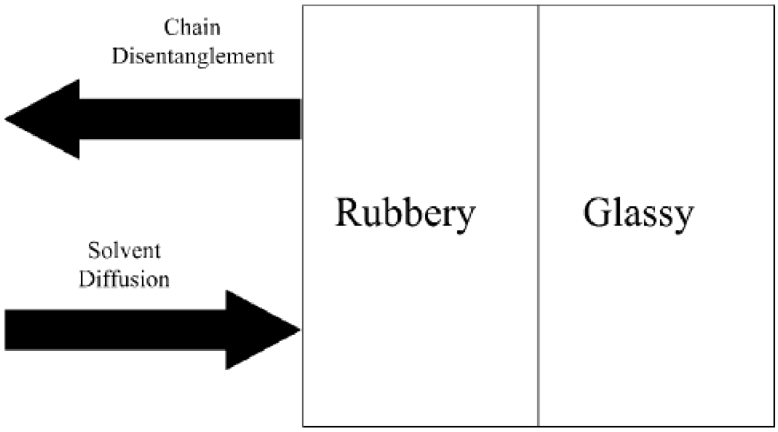

Figure 2.10: Solvent diffusion and polymer dissolution kinetics [50].

As it can be seen from the figure above, two interfaces are formed when a polymer starts to dissolve. The first one is between the rubbery and solvent phases. It is observed when the disentanglement and swelling of polymer chains are occurred. The second interface lies between the rubbery and glassy phases where the solvent cannot penetrate deeply into the polymer. The Figure 2.11 shows the interfaces in detailed from the pure polymer to pure solvent. The layers are in the order as: pure polymer, infiltration, solid swollen, gel, liquid layer and pure solvent, respectively. The first layer after solvent was applied to pure polymer is called infiltration layer where the rubbery phases of polymer is absorbed the solvent into its free volume in it. After filling the free spaces, the polymer still has a glassy structure however, the diffusion of solvent takes place so interaction between polymer and solvent increases.

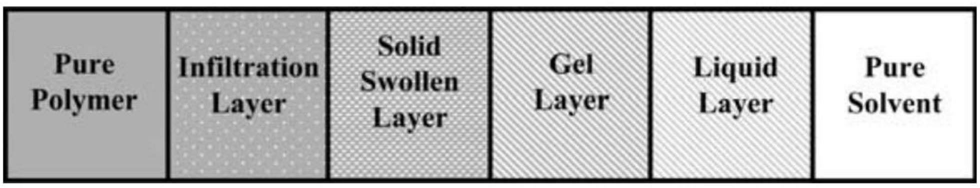

Figure 2.11: Formation of layers when dissolution process takes place [50].

The next step is forming the gel layer. In this part, glassy polymer becomes like a rubbery phase as in the figure. Liquid layer and pure solvent follow the order, respectively.

2.2.2.3 Degradation mechanism of PCL

Polycaprolactone tends to degrade in bulk degradation mechanism where the diffusion of water or environment is higher than hydrolysis reaction of polymer bonds. The reason of bulk degradation tendency is having ester bonds in polycaprolactone structure. As it is mentioned before, the rate of degradation depends on crystallinity of polymer, length of chains, molecular weight, hydrophilicity and hydrophobicity of biodegradable polymers. In addition, the hydrophilicity and hydrophobicity of polymers depend on the bonds and functional groups the polymers have. Degradation rate increases with decreasing length of chains, molecular weight and hydrophilicity of polymers [51]. After the bulk erosion, reduction in mechanical properties occurs and the mass loss remains still until a critical point. Because of semi-crystalline structure of polycaprolactone, the dashes line in the figure below can be followed up when the bulk degradation takes place. The degradation order is that first water diffuse into the bulk and after that, hydrolysis of ester bonds happens. In the following step, both low molecular weight polymers crystallize and water-soluble oligomers generate. The reason for the increase in crystallinity is that the amorphous parts first degrade and the crystalline regions remain. Also, since degradable polymers are easier to align, an increase in crystallinity is observed. As a result, the crystallinity increases and small degradation products like oligomers and monomers diffuse throughout the polymer. While these reactions occur, the physical and mechanical characteristics of polymer change. In the final part, reduction of mass is observed after decrease in molecular weight [52, 53].

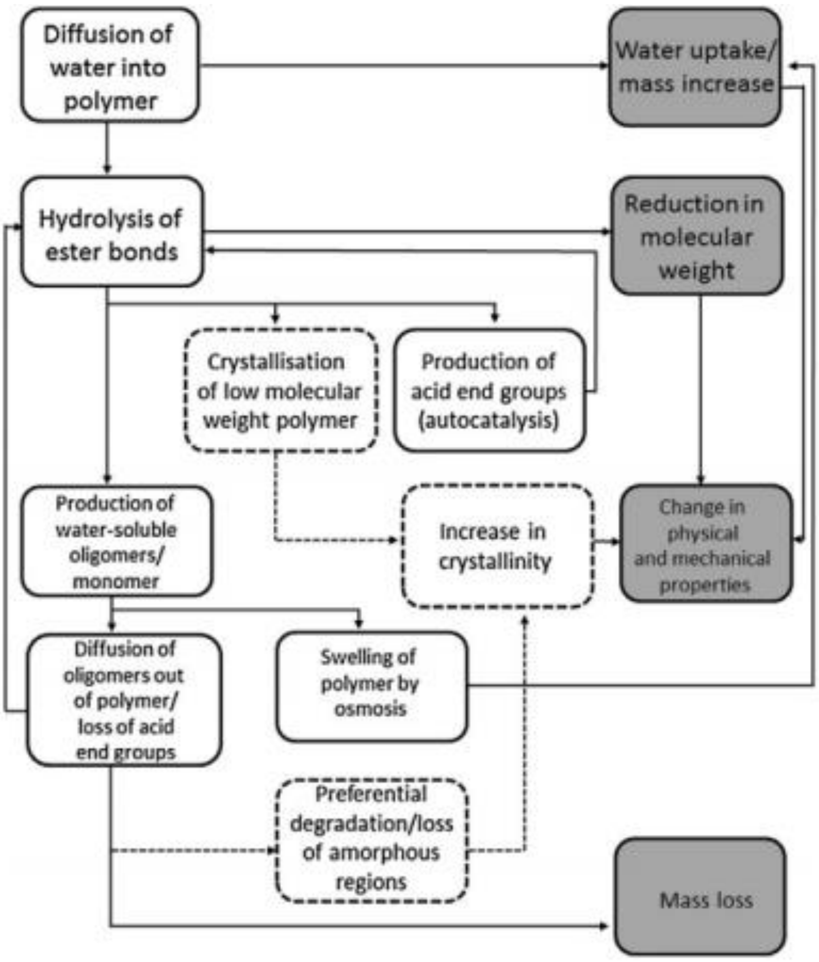

Figure 2.12: Bulk degradation mechanism step by step [52].

PCL has an intrinsic hydrophobic structure which results in a slow degradation. These degradation phenomena can be counted as both an advantage and disadvantage due to the application. The rate of degradation and growth of tissue must be similar to have a coherent healing time which is a significant parameter in tissue engineering. Otherwise, second surgery will be inevitable in this case. Rate of degradation can be adjusted by changing the molecular weight or length of polymer chain, amount of crystallinity and the environment in which the material is immersed [49]. These parameters all depend on techniques that are used, precursors during the polymerization process and different conditions such as temperature, pH and catalysts. When PCL and the other biodegradable polymers are compared, PCL is more durable because the number of its ester bonds in the polymer structure is fewer and it results in slow degradation rate for example 2-3 years in human body [10, 54-56]. The time of degradation can be arranged by changing thickness of polymer, pH of environment, usage of catalyzes and temperature. Eventually it will degrade into biological products. When PCL degrades into oligomers and monomers, the degradation product will be caproic acid which decreases the pH of medium and accelerates the rate of reaction. Afterwards, the products go into citric acid cycle. The last part is to eliminate of degradation products of body as seen in the Figure 2.13 (a).

The degradation mechanism and evaluation of PCL are demonstrated in the part b of the figure. Diffusion of water into amorphous phase is much easier and the degradation rate is higher than crystalline phase.

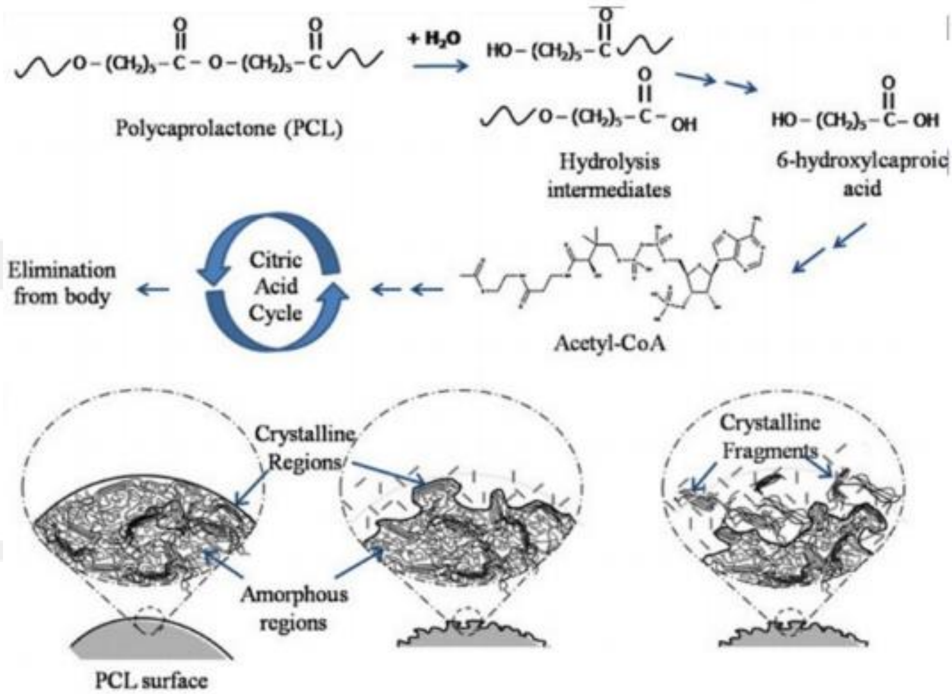

Figure 2.13: Schematics of hydrolytic degradation mechanisms of PCL [57].

2.3 Effect of Parameters for Degradation

The parameters affect the degradation rate is not differing from each other as in the dissolution and controlled drug release sections. Temperature, pH, time and pressure are the mutual ones in all of them. As the temperature and time increase the degradation rate increases and influence of pH can be varying according to polymers, enzymes and medium. In addition to these parameters, coating methods and micro arc oxidation process can be effective in the degradation process. Coating methods are divided into three main categories in this section such as spray coating, spin coating and dip coating. The reason of existence of coating methods as a degradation parameter is that degradation is influenced by obtaining a uniform, regular and continuous coating and also influenced by the thickness of coating. In addition, adhesion between the coating material and coated substrate also acts as a significant role in degradation rate. The degradation rate of the polymer decreases as the attachment of substrate and polymer increases. Improving the adhesion can be obtained by penetration of the polymers into porous substrate structure as in micro arc process [58].

2.3.1 Coating methods

2.3.1.1 Spray coating

Spray coating is a method in which a small drop of coating material is sprayed onto a base material by a nozzle with a pressure to form a thin film. The coated film layer is formed when the solvent is evaporated completely.

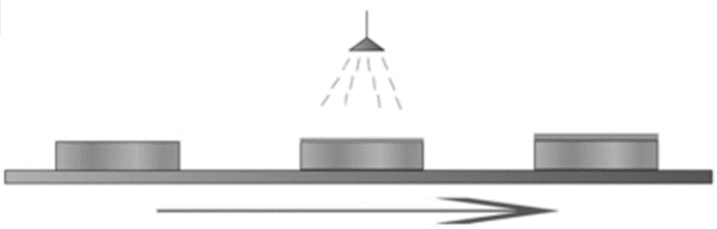

Figure 2.14: Spray coating method [59].

Nozzle to substrate distance, solvents effects, and pressure and substrate temperature are the main parameters which has remarkable influences on the spray coating [60].

There are many positive aspects which can be listed as: capability of coating large area, ability of coating complex shapes, minimum waste of coating material and budget-friendly equipment. However, obtaining a uniform coating is a downside of this method. Spherical nature of droplets and pinholes or cracks makes the distribution more difficult to achieve uniformity [61].

2.3.1.2 Spin coating

Spin coating process is obtained when excess amount of coating material is placed on the base material and then started to rotating at high speeds in order to use centrifugal force. When the whole the surface is covered with coating solution and drying is completed, the process is completed in three main stages. The thickness of film layer can vary depending on the viscosity and concentration of the coating material and the solvent. Other parameter that can affect the thickness is angular speed of spinning.

There is a reverse proportion between angular speed and the thickness. The thicker film is formed with the decreasing in angular speed [62].

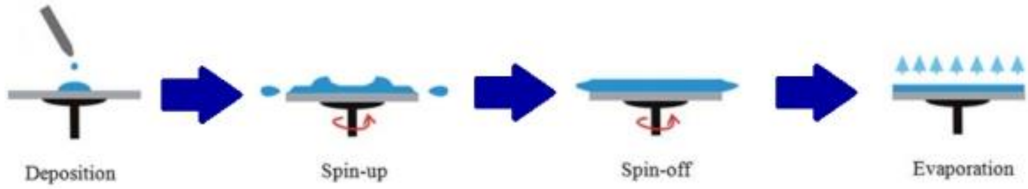

Figure 2.15: Steps of spin coating method [63].

There are some advantages of spin coating which can be listed as: a suitable process for all types of substrates, a mature technique and a process forms homogeneous films in a short time. On the other hand, incomplete coverage of complex geometries, possibility of crack and chuck marks can be listed as disadvantages of this method [64].

2.3.1.3 Dip coating

Dip coating is the simplest and oldest process where the substrate is dipped into desired coating solution and coating is obtained after drying processes. It is a one of the types of sol-gel coating methods at atmospheric conditions and controlled temperatures. Dip coating consists of five stages which are immersion, start-up, deposition, drainage and evaporation, respectively. Immersion is the first step that the specimen is soaked into coating solution at a constant speed. While the substrate is immersed into a solution, a boundary layer is generated due to fluid mechanics. After that, the whole specimen is kept in the solution for a while and then pulled out. In the third step, deposition of a solution on the surface of substrate is formed when lifting is started. There is an important parameter in this stage which called as a “withdrawn speed”. This speed plays an important role in the thickness of coating. When the speed increases, the thickness of coating also gets thicker. Also, withdrawn speed is a constant speed to prevent some problems such as jitter. From this moment, boundary layer separates the inner and outer layers from each other where the inner one moves with direction of substrate and outer layer with excess solvent goes into solution [65, 66]. Then, drainage is the step where the excess of solution is removed by gravity forces. The last step is evaporation of the solvent to generate a uniform and homogeneous layer [67].

Coating can be affected by different forces which are gravity, surface tension force and fractional force between solution and the substrate.

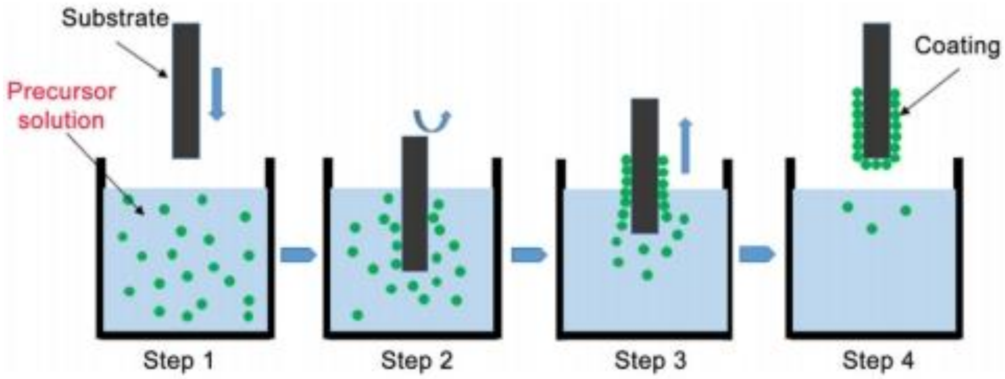

Figure 2.16: Steps of dip coating process. Immersion, start-up, deposition & drainage and evaporation, respectively [66].

Obtaining a thin and uniform layer depends on the type of substrate's surface, viscosity of coating material and withdrawn speed. In dip coating process, deposition is obtained faster depending on the type of solvent is used when compared to other deposition techniques [68]. Other advantage of this process is being costly effective and the ease of using variety of chemicals. As it mentioned before, withdrawn speed can determine the thickness of coating by using Landau- Levich equation [69, 70]. This equation shows that there is a direct proportion between withdrawn speed and the thickness.

$$h = 0.94\frac{(\eta U)^{2/3}}{\gamma^{\frac{1}{6}}(\rho \mathrm{g})^{1/2}} \tag{1}$$

•h: Thickness of coating

•η: Viscosity of liquid

•U: Withdrawn speed

•γ_{LV}: Surface tension

•ρ: Density of solution

•g: Gravity

It is known that there are varieties of application areas of dip coating. For example, it is used in hydrogels, adhesive and pharmaceutical caplets besides in sol-gel applications [71-73].

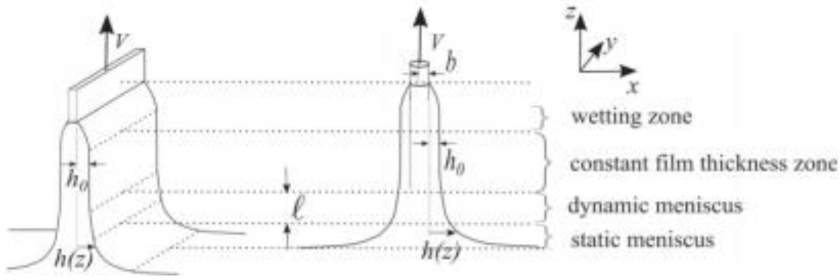

Figure 2.17: Dip coating regions based on Landau- Levich equation [69].

Four regions have been identified as major parts of dip coating processes which are the static meniscus, the dynamic meniscus, the constant thickness zone and the wetting zone. Where the wet film is observed at the first sight, the region is called wetting zone. After that, the thickness of wet film is reached a given thickness in constant thickness zone. In the static meniscus region, balance of hydrostatic and capillary pressures designates the shape of meniscus. Finally, when the entraining and draining forces achieves the equilibrium point, the stagnation is obtained which can be called as dynamic meniscus [69].

2.3.1.4 Micro-arc oxidation (MAO)

Micro arc oxidation is an anodic oxidation process with applied high voltage. MAO is also known as spark anodizing, anodic spark deposition, micro arc anodizing, micro-plasma anodizing and electro-plasma deposition. Micro arc oxidation system consists of an anode, a cathode, a stirrer, an electrolyte, a cooling system and a power supply as it can be seen from Figure 2.18 [15]. In this process, the anode is the sample to be coated as a result of the MAO method. In addition, although the set up components are given in the figure in general terms, these parameters may vary according to the desired coating in each experiment.

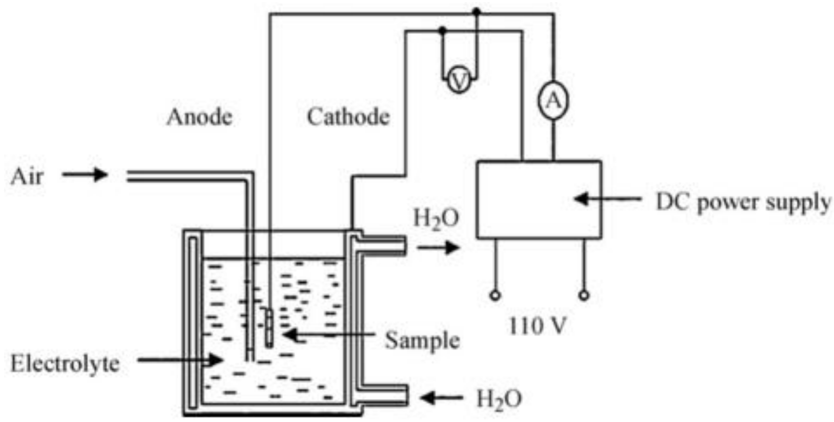

Figure 2.18: Components of micro-arc oxidation process [74].

The process begins with the immersion of anode which is the substrate wanted to be coated in the electrolyte. Then, applied voltage is increased rapidly by the time and the passivating film is observed on the substrate. When the applied voltage is increased, some oxygen bubbles are seen and the oxidized film is generated. At some point, the voltage will be surpassed the dielectric breakdown of generated oxidized film and micro-arc discharges are formed. In the meantime, elements from the electrolyte and the substrate are diffused into this breakdown region at high temperature and micro-arc discharges are transformed into plasma discharges which have higher glowing and sparkling. New oxidized coating is formed on the surface and with the increasing oxidation time and applied voltage the porous structure is obtained through the whole surface. Finally, porous ceramic oxide layer is covered all the surface of the specimen.

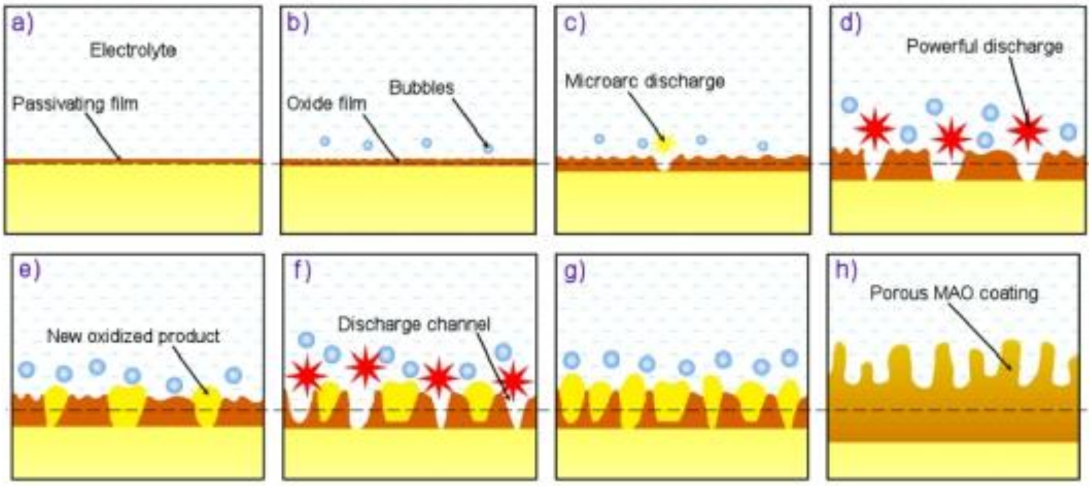

Figure 2.19: Steps of micro-arc oxidation process [15].

The morphology of the surface such as smooth, rough, spherical porous, or irregular porous can be obtained by differing the parameters of the MAO process. These parameters can be listed as composition of electrolyte, oxidation time, applied voltage and current. Adjusting the composition of MAO electrolyte plays a significant role on the porosity, behavior of the surface and the thickness of the coating and electrolyte is chosen due to the usage area. For example, antibacterial agents such as silver, platinum, zinc and copper are used in electrolytes for biomedical applications. MAO is also used for increasing the wear resistance, corrosion resistance and heat resistance.

Moreover, it is reported that micro arc oxidation process can be used to increase the adhesion between the base metal and the coating material. The reason is because the obtained porous structure after MAO process can absorb the coating and due to the penetration and electrostatic interaction between the base and coating layer, an improvement in adhesion strength can be observed [75]. Yu-Kyoung Kim et al. [75] concluded that micro-arc oxidation also known as plasma electrolytic oxidation is applied in order to improve the adhesion between coating layer and base material. The base material was chosen as magnesium and coating material was polycaprolactone to increase the corrosion resistance of magnesium. They concluded that the experiment results promised hope for industrial applications due to increase the corrosion resistance of magnesium by coating polycaprolactone on micro arc oxidation applied magnesium samples.

Additionally, as it was mentioned before, porous ceramic oxide layer formed on sample's surfaces after micro arc oxidation was applied and it was ended up with increment in corrosion resistance. Long-Hao Li et al. [76] studied a coated thing consists of polycaprolactone and micro-arc oxidation process to prevent the corrosion of magnesium implant material. 4-7% PCL solution (dichloromethane as a solvent) were coated on the porous magnesium oxide surface by dip coating method. Hence, the results showed that with the increase in the polycaprolactone percentage, the quality which are regularity, corrosion resistance and thickness of coating and ability to cover all the porous surface were increased as seen in the Figure 2.20. The left side of the Figure 2.20 shows SEM images of the surface and, in the right side images, represents the cross sectional areas of the samples coated with 4% and 7% PCL solution. As a result, 7% PCL solution was chosen because it closes all pores and increases the corrosion resistance of magnesium, which will be used as a dental implant.

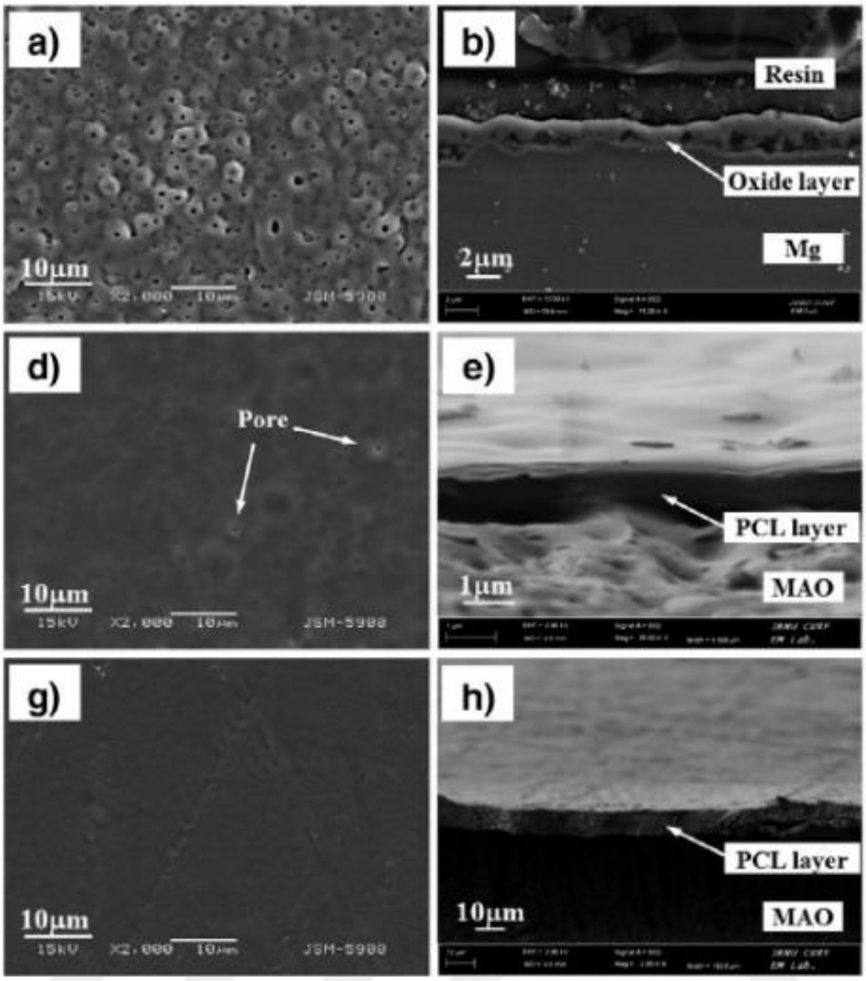

Figure 2.20: Surface characteristics (a, d, g) and cross-section figures (b, e, h) of the MAO coated and MAO–PCL duplex coated Mg: (a, b) MAO coated Mg, (d, e) MAO–4PCL duplex coated Mg and (g, h) MAO–7PCL duplex coated Mg.

Furthermore, micro arc oxidation is applied not only for improving the corrosion resistance and adhesion strength between base and coating layer, but also providing the possibility of controlled drug release. The reason for this is that the electrolyte can be changed as desired in the micro arc oxidation process and the material to be doped is added to the electrolyte content. Xiao Hong Yao et al. [77] investigated the copper effect on antibacterial properties of micro-arc coated titanium. They stated that the shiny parts surrounding the porous structures indicate the doped copper. Also, they concluded that the doping metal ions entrapped into porous structure to have a controlled drug release and show sustainable antibacterial release. The findings showed that copper has an antibacterial influence on E. coli and S. aureus bacteria so antibacterial feature of Ti was increased.

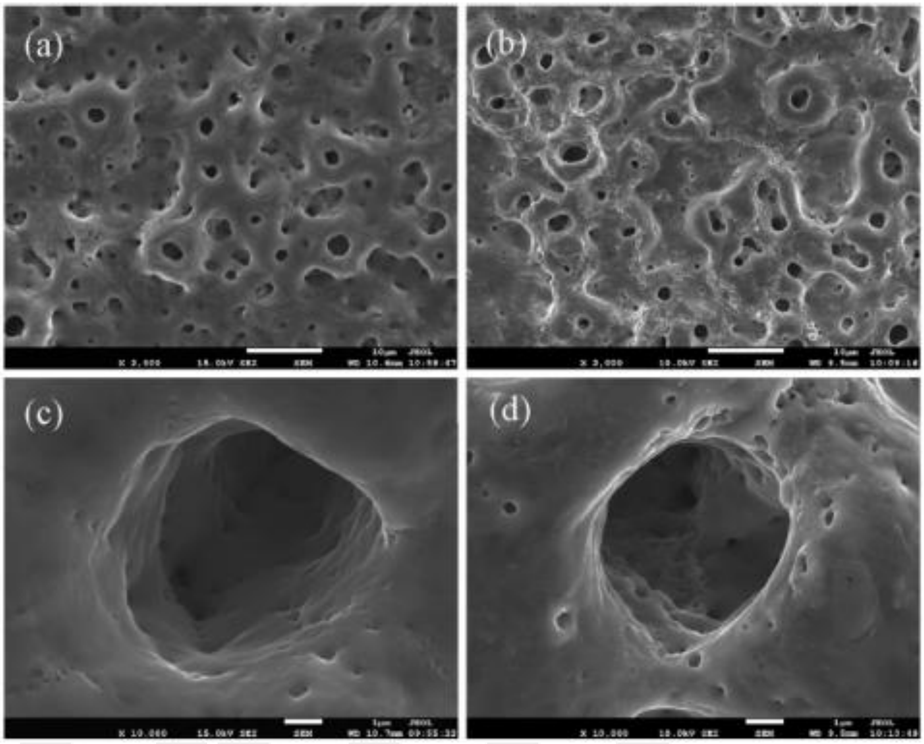

Figure 2.21: Surface SEM micro-graphs of Cu-free (a, c) and Cu-doped coatings (b, d) [77].

It can be concluded that micro arc oxidation is an effective process in order to increase the corrosion and wear resistance and sustain a controlled drug release with a porous structure.

2.4 Implant Materials

Choosing the right biomaterial to cure or heal a disease plays a crucial role in humans' health. An ideal biomaterial should have following properties; preventing inflammatory as body implants, coherent degradation time with healing part, matching mechanical properties and having non-toxic by-products [78]. There are some metals and alloys used as implant materials such as stainless steel, cobalt base alloys and titanium alloys. Among these materials titanium and its alloys have become one of the most common materials for biomedical applications because of meeting the requirements of biocompatibility, high resistance of corrosion, antibacterial ability and their strength. Moreover, having a light density (4.5 g/cm^3) can be count as a benefit for implant materials [79]. Yazdani et al. [80] confirmed that titanium implants show better biocompatibility compared to zirconia because of preventing corrosion layer between the implant and bone. The reason of being biocompatible is the presence of titanium oxide film on the surface. Furthermore, Acero et al. [81] observed that Ti has a good corrosion resistance and desired osseointegration characteristics for biomedical applications. Osseointegration behavior of Ti which means the attachment of implant to the bone (Figure 2.22) [80].

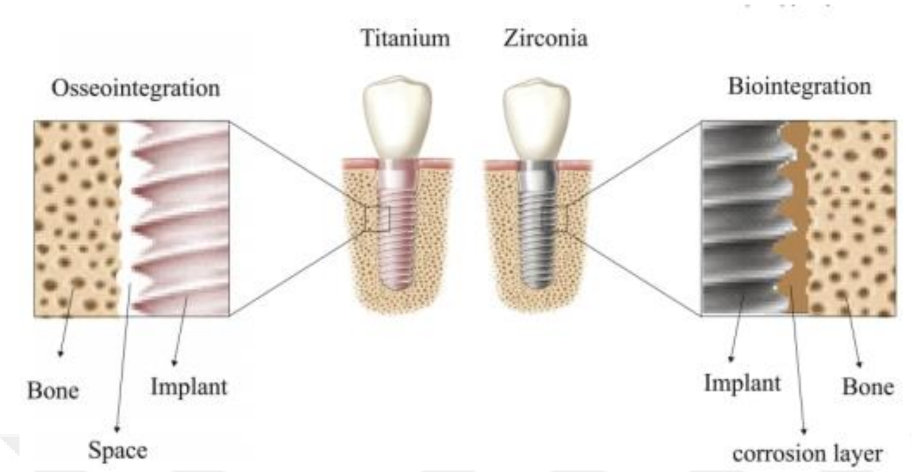

Figure 2.22: Osseointegration and biointegration behavior of titanium and zirconia implants.

Another reason which makes Ti a better candidate is that the difference of Young Modulus between bone and implant material is lesser than the others. Bone and teeth has approximately 13 and 20 GPa, respectively. Figure 2.23 compares the Young Modulus of different type of dental implant materials.

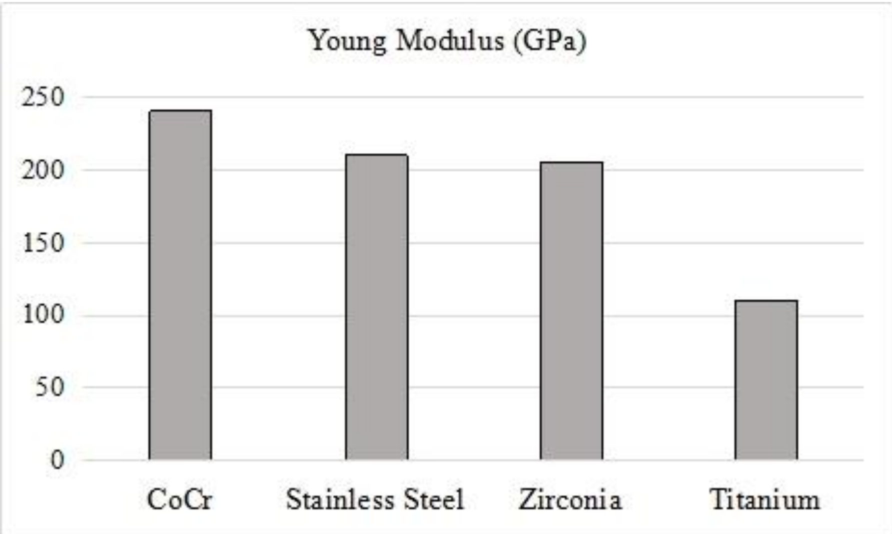

Figure 2.23: Comparison of Young modulus of implant materials [12].

The result of this difference can be defined as stress-shielding phenomenon. Wear and loosening of the implant, refracturing and non-healing of a bone can be the reasons of the mismatching between the Young modulus. Moreover, to overcome this phenomenon, some solutions are specified. In addition to choosing the ideal material, adjusting the size and the shape of the implant and having an implant material with a porous structure can minimize this problem. To sum up, titanium is one of the best candidates as an implant material due to its superior properties.

2.4.1 Titanium

For dental applications, titanium and its alloys are widely chosen. As mentioned before, Ti and its alloys are materials with high corrosion resistance and antibacterial properties. In addition, they are biocompatible materials thanks to the titanium oxide layer they form on the surface. Titanium can be as a commercially pure (Grade 1 to 4) or two alloys such as Ti6Al4V and Ti6Al4V ELI according to ASTM Committee F-4 for Surgical Implants. The alloying elements can increase the strength and toughness; reduce the Young modulus or brittleness. However, alloying elements such as vanadium, copper and tin can be toxic and hazardous for human body. So, commercially pure titanium should be selected based on its content of elements and mechanical characteristics.

Table 2.2: Content of elements for Grade 1 to 4 (ASTM F 67).

Element	Grade 1	Grade 2	Grade 3
N max	0.003	0.003	0.05
C max	0.1	0.1	0.1
H max	0.015	0.015	0.015
Fe max	0.2	0.3	0.3
O max	0.18	0.25	0.35
Ti	Balance	Balance	Balance

As it is can be seen from the table above, presence of oxygen in Grade 4 is higher than the rest. The amount of oxygen determines the mechanical properties such as elongation, yield and tensile strengths.

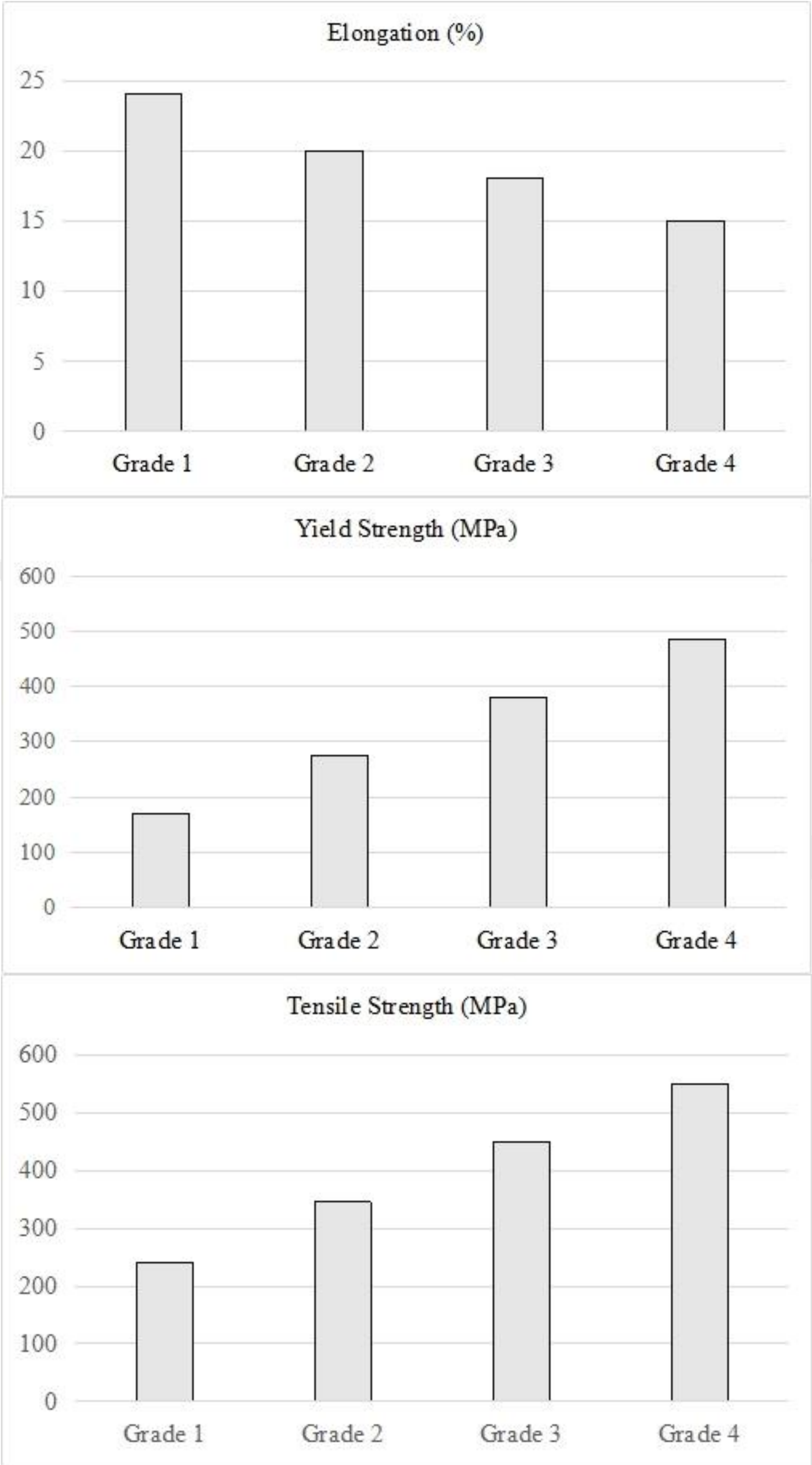

Figure 2.24: Comparison of mechanical properties (a) Young modulus, (b) yield strength and (c) tensile strength of CP Ti (Grade 1 to 4) [13].

Grade 4 Ti is selected for dental implants because of its the mechanical and biological properties. In addition, according to McCracken et al. [12] most of dental implant manufacturers chose Cp 4-Ti which is shown in the Figure 2.25.

	cp Ti Grade I	*cp Ti Grade II*	*cp Ti Grade III*	*cp Ti Grade IV*
3i	*	*	X	
BioHorizons				
Lifecore			X	X
Nobel Biocare	X			
Paragon				X
Steri-Oss				X
Sulzer Calcitec				

*3i company representatives use materials that meet cp grade I and grade II specifications, but that are cold-worked to improve yield strength

Figure 2.25: Commercial demand of implant material in dental applications [12].

Le Guéhennec et al. [82] studied on surface modification of titanium to improve bone adhesion in dental applications. Osseointegration behavior influences by roughness of surface and their composition. They concluded that there are some methods such as titanium plasma-spraying, etching with acid, micro arc anodization (MAO) or calcium phosphate coatings which can improve the osseointegration as the its roughness increases. Moreover, increasing in adhesion and bonding between substrate and attached material with enhanced roughness is a known fact [83,84]. However, there are some situation that are not desired to be attached to specimen. For instance, generation of bacteria is one of the cases which is a crucial circumstance in dental applications. Yeo et al. [85] emphasized that formation of bacteria also increases as the roughness increases. As it was mentioned before, antibacterial agents can be used to inhibit and minimize the formation of bacteria under this circumstances.

3. EXPERIMENTAL PROCEDURE

3.1 Materials

Cp-Ti (Grade 4) was used as the base substrate. MAO electrolyte consists of calcium acetate ($Ca(C_2H_3O_2)_2$, VWR BDH Prolabo), sodium hydroxide (NaOH) and silver acetate (CH_3COOAg, Alfa Aesar). In order to investigate the effects of viscosity on thickness and degradation, different weight percentages of PCL were used (1.5 and 10%). PCL (M_w: 80,000 Da) was supplied from Sigma-Aldrich, USA. Solvent of PCL was chosen as chloroform ($CHCl_3$, Sigma-Aldrich). Moreover, to increase the degradation rate of PCL, $SnCl_2$ (%100, Merck) was used as a catalyst. $SnCl_2$ was used the amount of 5% wt of PCL.

3.2 Preparation of Dublex Coated Ti

Cp-Ti Grade 4 stick was cut into a disc shape with dimensions of 12 mm diameter and 4 mm height used as the base substrate. The Ti specimens were mechanical ground up to 2500-grit with SiC coated abrasive paper. Then, they were cleaned using ethanol, acetone and distilled water in an ultra-sonic cleaner for 5 minutes. The MAO process was done by using 20.5 g/L $Ca(C_2H_3O_2)_2$ and 3 g/L NaOH at limiting voltage of 400 (+) V 60 (-) V for 3 min. Also, silver was introduced in the form of 0.004 M CH_3COOAg. 1, 5 and 10 wt.% PCL solutions were used and they were prepared by dissolving the required amount of PCL in $CHCl_3$ by stirring for 2 h in order to have a homogenous solution. The best coating solution was achieved by 5% wt. PCL (95% wt. $CHCl_3$) due to its ideal viscosity to have homogeneous solution and coating thickness. After choosing the right amount of PCL, $SnCl_2$ was added into dip coating solution as catalyst to increase the degradation rate of PCL. Since higher than 8 ppm tin has toxic effect tin human body, its amount was determined as 5% of PCL amount to eliminate the toxicity. The PCL coating was obtained by dip coating method (Figure 3.1). The MAO treated Ti samples were immersed in the PCL solution for 1 minute and they were pulled out at a rate of 20 mm/min followed by drying at 40 °C for 12 hours. The silver doped MAO treated Ti sample coated with 5 wt. % PCL solution was labeled as Ti-TiO_2-Ag-5PCL where the uncoated was Ti-TiO_2-Ag.

Figure 3.1: Dip coating instrument (KSV NIMA Dip Coater).

To examine the effect of PCL coating on release of silver, both coated and uncoated samples were placed in SBF. The volume of SBF was equal to 100 times total surface area of disk according to standard. SBF was prepared according to BS ISO 23317:2014 - Implants for surgery — In vitro evaluation for apatite-forming ability of implant materials standard. Na^+, K^+, Mg^{2+}, Ca^{2+}, Cl^-, HCO_3^-, HPO_4^{2-}, SO_4^{2-} ions were adjusted to have a good SBF solution where the temperature was 37°C and pH was 7.4.

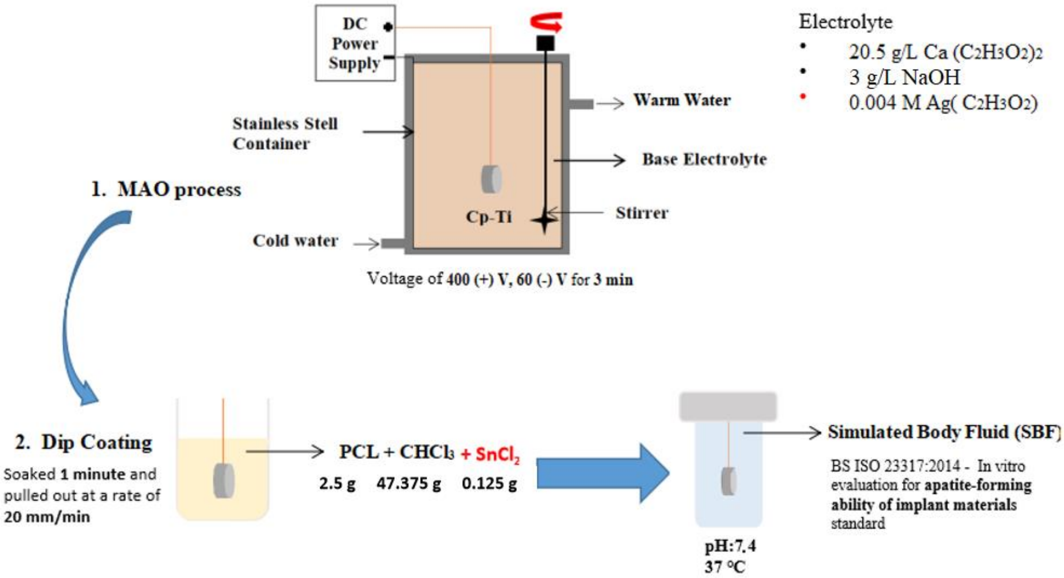

Figure 3.2: Schematic representation of experimental procedure.

After preparation of SBF, samples were soaked into 37,7 ml SBF for 1,2, 3 and 4 weeks. In this system, 2 specimens were set up for each week, 8 in total, in order to characterize both at the surface and cross sections from each sample.

Table 3.1: Experiment procedure.

Specimen	Time in SBF
Ti-TiO_2-Ag/ SBF	First week and 14th, 21st, 28th days
(1) Ti-TiO_2-Ag- 5PCL_{SnCl2}/ SBF	1 week
(2) Ti-TiO_2-Ag- 5PCL_{SnCl2}/ SBF	2 weeks
(3) Ti-TiO_2-Ag- 5PCL_{SnCl2}/ SBF	3 weeks
(4) Ti-TiO_2-Ag- 5PCL_{SnCl2}/ SBF	4 weeks

3.3 Characterization

3.3.1 Morphological analysis

3.3.1.1 Optical microscope

Optical microscope (Nikon ECLIPSE LV150L) was used in order to observe the HA formation on surface. The magnification range is between 5x to 100x.

Figure 3.3: Optical microscope (Nikon ECLIPSE LV150L).

3.3.1.2 Scanning electron microscopy (SEM)

Scanning electron microscopy (SEM, Hitachi TM-1000, Jeol JSM-6510 and Jeol NeoScope JCM6000) equipped with EDS was used to examine the distribution of pores formed as a result of the micro arc oxidation process and the morphology of the structures formed by silver dopping.

3.3.2 Chemical analysis

3.3.2.1 X-ray diffactometer (XRD)

XRD studies were carried out with (GBC, MMA 027) equipped with Cu−Kα radiation and the 2θ range was between 10−90°. X-ray diffraction analysis (XRD) was used to characterize the phase composition of TiO_2 and silver compounds.

3.3.2.2 Gel permation chromatography (GPC)

A common non-polar solvent is tetrahydrofuran (THF) (99.99% Merck) was used in gel permeation chromotography for detection of PCL molecular weight. GPC was performed by Shimadzu equipped with a RID-10A refractive index detector. THF was used as the elution solvent at a flow rate of 1.0 mL/min and the columns were equilibrated and run at 30 ^{o}C.

3.3.2.3 pH analysis

The pH analysis (WTW portable pH meter ProfiLine pH 3110) were carried out to measure the change in the pH of SBF caused by the degradation of PCL and formation of HA at the constant body temperature 37^{o}C after 28 days.

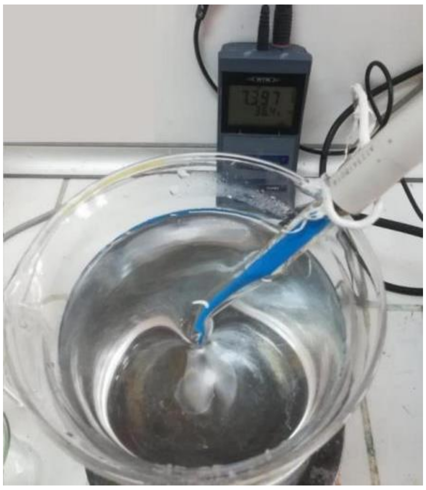

Figure 3.4: The pH analysis (WTW portable pH meter ProfiLine pH 3110).

3.3.2.4 Fourier infrared spectroscopy (FTIR)

FTIR spectra were performed by a Bruker Tensor 27 FTIR spectrometer with a diamond crystal single reflection ATR universal plate. FTIR Analysis was used to evaluate the degradation of PCL, its degradation products and hydroxyapatite in wavenumber range 400-4000 cm^{-1}.

3.3.2.5 Atomic absorption spectroscopy (AAS)

AAS (PinAAcle™ 900F) was performed to determine the amount of silver release from week 1 to week 4 by using silver lamp.

Figure 3.5: AAS (PinAAcle™ 900F) to determine the amount of silver release.

4. RESULTS and DISCUSSION

4.1 Morphological Analysis

4.1.1 Optical microscope

The difference of macroscopic structure among Ti-5PCL, Ti-TiO_2-5PCL /SBF and Ti-TiO_2-Ag-5PCL/SBF were evaluated by optical microscope. As can be seen from Figure 4.1, it was observed that PCL coated on Cp-4 Ti without the MAO treatment did not stick on the sample after it was soaked in SBF. It is believed that the porous structure of MAO and electrostatic interactions between carboxylate group of PCL and Ti surface caused a better adhesion between the Ti and coating. Also, when examined macroscopically, it was seen that there were yellowish spots on Ti-TiO_2-Ag due to silver doping by MAO process (Fig.4.1(b) sample on the left).

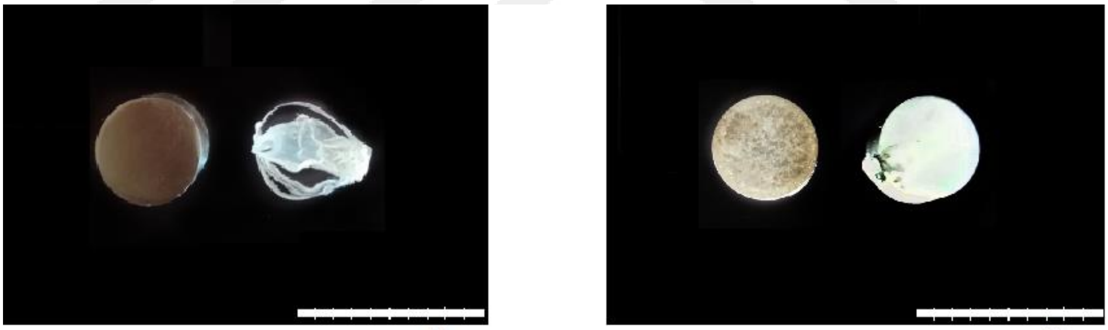

(a) 20 mm (b) 20 mm

Figure 4.1: Importance of MAO process on the adhesion of PCL coating (a) Ti-5PCL non-adhesion between coating and Ti, (b) Ti-TiO_2-Ag-5PCL/SBF and Ti-TiO_2-5PCL /SBF.

Moreover, both Ti-TiO_2-Ag-5PCL and Ti-TiO_2-Ag-5PCL/SBF showed the formation of spherulites as can be seen in Figure 4.2- After 1 week. This type of formation can be seen when crystallization of polymers happens from the bulk instead of from solution and as a result these spherical structures are called spherulites. Visible changes in the surface properties of the samples were observed after they were soaked in the SBF solution. The reason for these changes can be demonstrated by the degradation of the PCL in the SBF and formation of amorphous biomimetic HA.

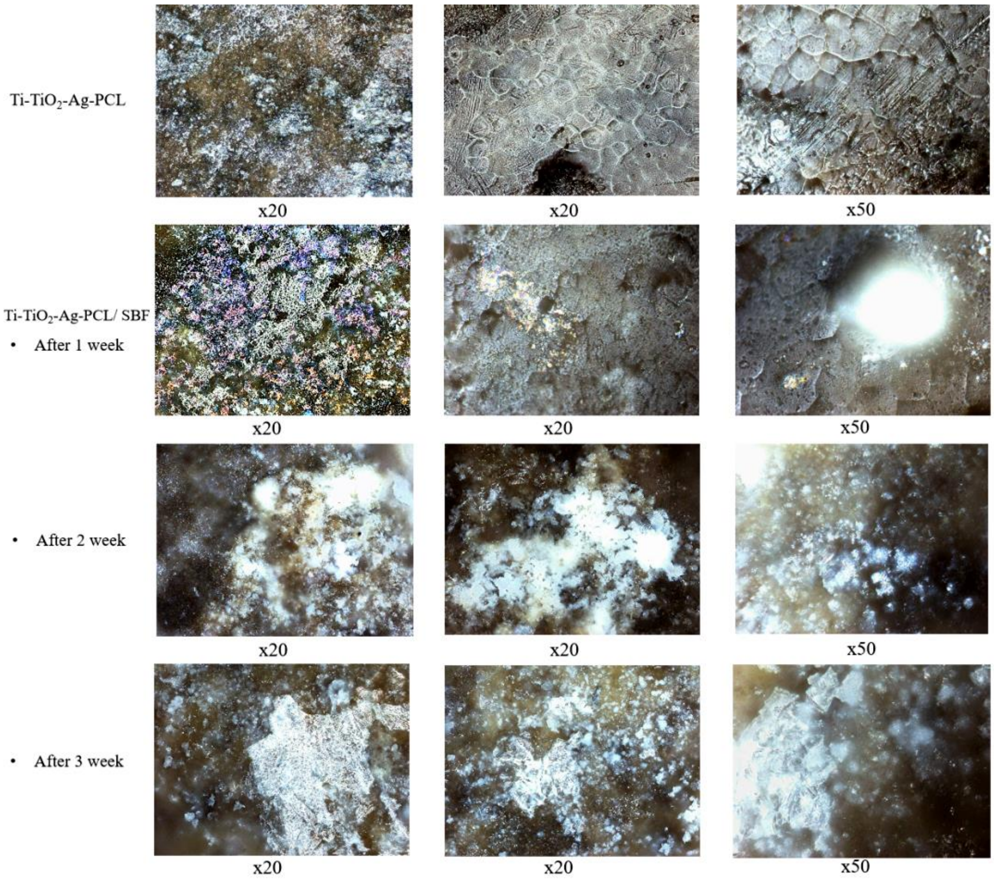

Figure 4.2: Comparison of optical images of Ti-TiO_2-Ag-PCL_{SnCl2} before and after soaked in SBF.

Different colors were observed due to the refraction of light as a result of the degradation of the polymer. Moreover, there was a decrease or deterioration in the amount of spherulite formed. At the end of the first week, as can be seen in the x50 image, very bright spots were scattered in certain places which indicated the amorphous biomimetic HA. Biomimetic HA is formed by the accumulation of calcium and phosphate contained in SBF. It was observed that the amount of formation of biomimetic HA on the surface increased.

It was also seen that the amorphous biomimetic HA seemed like a crystal structure over time (3rd week x50 image). Although the structure looks like a crystal, it shows an amorphous feature because of working temperature is 37 °C, not high temperature. As a result, it was concluded that the polymer in SBF degraded. The visuals of the 4th week were not included, as it became difficult to clarify the visuals in the optical microscope with the increase of biomimetic HA on the surface. The formation of biomimetic HA indicates that a structure compatible with the bone has been formed in vitro.

4.1.2 SEM analysis

Figure 4.3 shows the SEM image of Ti-TiO_2 at 2000 magnification. The morphology of MAO coated with Ti was spherical, regular and porous. The dark spheres indicated pores whereas the lighter regions belonged to TiO_2. The average pore size was calculated as 2.145 μm.

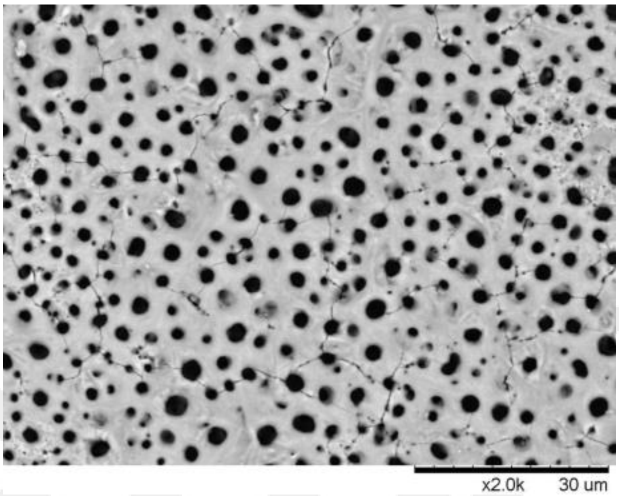

Figure 4.3 Ti-TiO_2 by SEM at 2000 magnification.

In order for the silver to be doped, the desired structure here was a regularly porous surface. Figure 4.4 demonstrates the morphology of Ti-TiO_2-Ag where the silver entrapped into the porous structure of TiO_2 at 1000 magnification. With the doping of silver, it was seen that new structures were formed. Generally, dendritic structures and white residues were observed on the surface. XRD and EDS characterizations were carried out for the detailed examination of these structures.

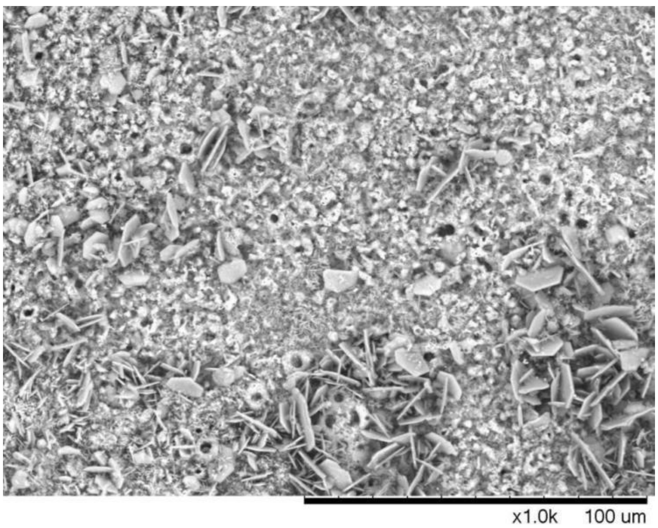

Figure 4.4 Ti-TiO_2-Ag / MAO by SEM at 1000 magnifications.

4.2 Chemical Analysis

4.2.1 XRD- EDS results

XRD and EDS analyses were performed to evaluate the phases of Ti-TiO_2/MAO and Ti-TiO_2-Ag/MAO specimens. In the appendices, the mass % of the EDS results belonging to the previous study are given in the presence of oxygen. The ratio of silver has been increased by 4 times to better see the silver release. In order to indicate the presence of silver in the new EDS results, silver is taken as a basis. As it can be seen from the Fig.4.5, XRD patterns show the presence of different phases of TiO_2 such as rutile and anatase. Also, peaks belong to Ag_2O and $CaTiO_3$ compounds were found since the MAO electrolyte contained Ca $(C_2H_3O_2)_2$ and CH_3COOAg. The peaks at 26°, 34°, 53°, 64° and 71° indicate rutile phase whereas the anatase peaks at 37°, 39°, 48° and 55°. Titanium peaks were seen at 35°, 51°, 62°, 70° and 74°. On the other hand, the peaks of Ag_2O were seen at 24°, 27.94°, 30°, 32,27° and 43°, while $CaTiO_3$ at 31°, 49° and 60°.

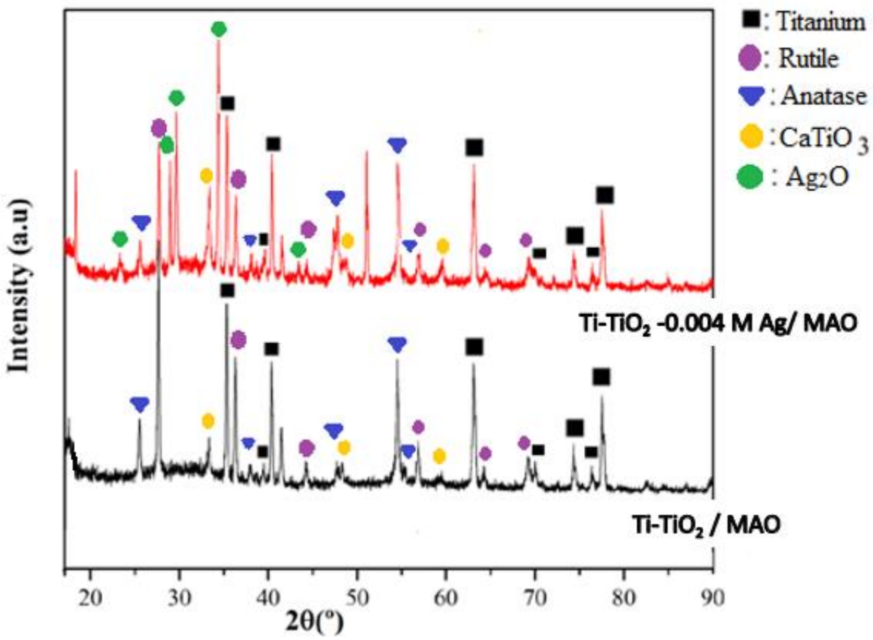

Figure 4.5: XRD results of Ti-TiO_2 and Ti-TiO_2-0.004 M Ag.

Moreover, in order to evaluate the effect of PCL coating on Ti-TiO_2-Ag and the changes of phases after soaking the samples in SBF for 1 to 3 weeks, XRD was performed. It was observed that biomimetic amorphous HA was formed after soaking in SBF. It is thought that the formation of biomimetic amorphous HA is the cause of the shift in titanium peaks and the decrease in the peak intensities.

It was also seen that biomimetic amorphous HA peaks were increased in Ti-TiO_2-Ag-PCL_{SnCl2}/ SBF 2 weeks and Ti-TiO_2-Ag-PCL_{SnCl2}/ SBF 3 weeks' spectra (Figure 4.6).

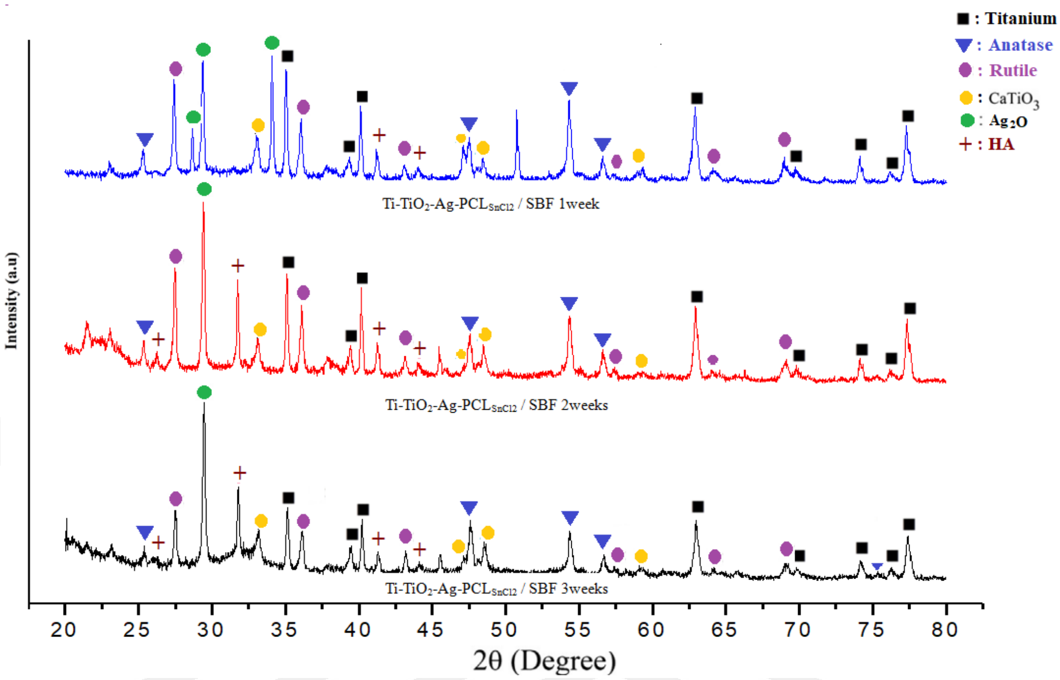

Figure 4.6: XRD results of Ti-TiO_2-Ag-PCL_{SnCl2}/ SBF 1 week, Ti-TiO_2-Ag-PCL_{SnCl2}/ SBF 2 weeks and Ti-TiO_2-Ag-PCL_{SnCl2}/ SBF 3 weeks.

In Figure 4.6, there are 4 peaks of the silver compound in the first week after immersion in SBF. Looking at the 2nd and 3rd week spectra of the samples immersed in SBF, it was seen that the peaks except the peak at 31° disappeared. The reason why the peak at 31° remains is that the (111) plane has a stable structure. The reason for the stability of the (111) plane is that the bond length between oxygen and silver is the shortest and it contains covalent bonds. The covalent bond causes that plane to be hydrophobic.

XRD results confirm the results of EDS analysis. As can be seen in Fig.4.7 a, b, c; 3 different types of structures were observed in EDS results: porous structures because of MAO process, needle shape structures and shiny sparkles due to silver doping. The follow up analysis was carried out in order to find out % weight of the elements and to confirm the possible compounds.

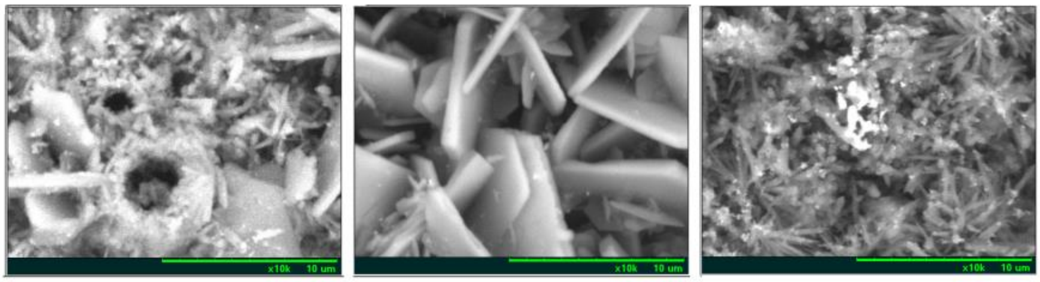

(a)		(b)		(c)	
Element	**Weight (%)**	**Element**	**Weight (%)**	**Element**	**Weight (%)**
Calcium	89.0	Calcium	95.5	Calcium	85.0
Titanium	6.5	Titanium	2.4	Titanium	2.6
Silver	4.5	Silver	2.1	Silver	12.3

Figure 4.7: EDS results and quantify spectrum.

As a result of EDS analysis, it was seen that the porous structure contained 89% Ca, 6.5% Ti, and 4.5% Ag, (Fig.4.7. (a)); needle shape structure contained 95.5% Ca, 2.4% Ti and 2.1% Ag, (Fig.4.7. (b)); whereas the structure with shiny spots contained 85% Ca, 2.6. % Ti and 12.3% Ag, (Fig.4.7. (c)).

4.2.2 GPC

Tin chloride was chosen as a catalyst to accelerate the degradation rate of PCL. Tin chloride was chosen as the catalyst because it has activity against polycaprolactone in SBF solution and tin's capacity to increase its the coordination number. The pre-experiments were done with different amounts of $SnCl_2$ with PCL pellets to examine the activity of $SnCl_2$ (Fig.4.8) in SBF solution. GPC characterization results in Fig.4.8 showed that the rate of degradation increased with the increase of $SnCl_2$ used as degradation catalyst. GPC peaks in the figure indicate the molecular weight of degraded PCL and the area under the peak shows the percentage PCL in the medium. Peaks other than peak 1 were considered as degradation products of PCL such as 6-hydroxy caproic acid and monomer. Peak 1 indicates the lower molecular weight PCL formed as a result of the degradation of PCL.

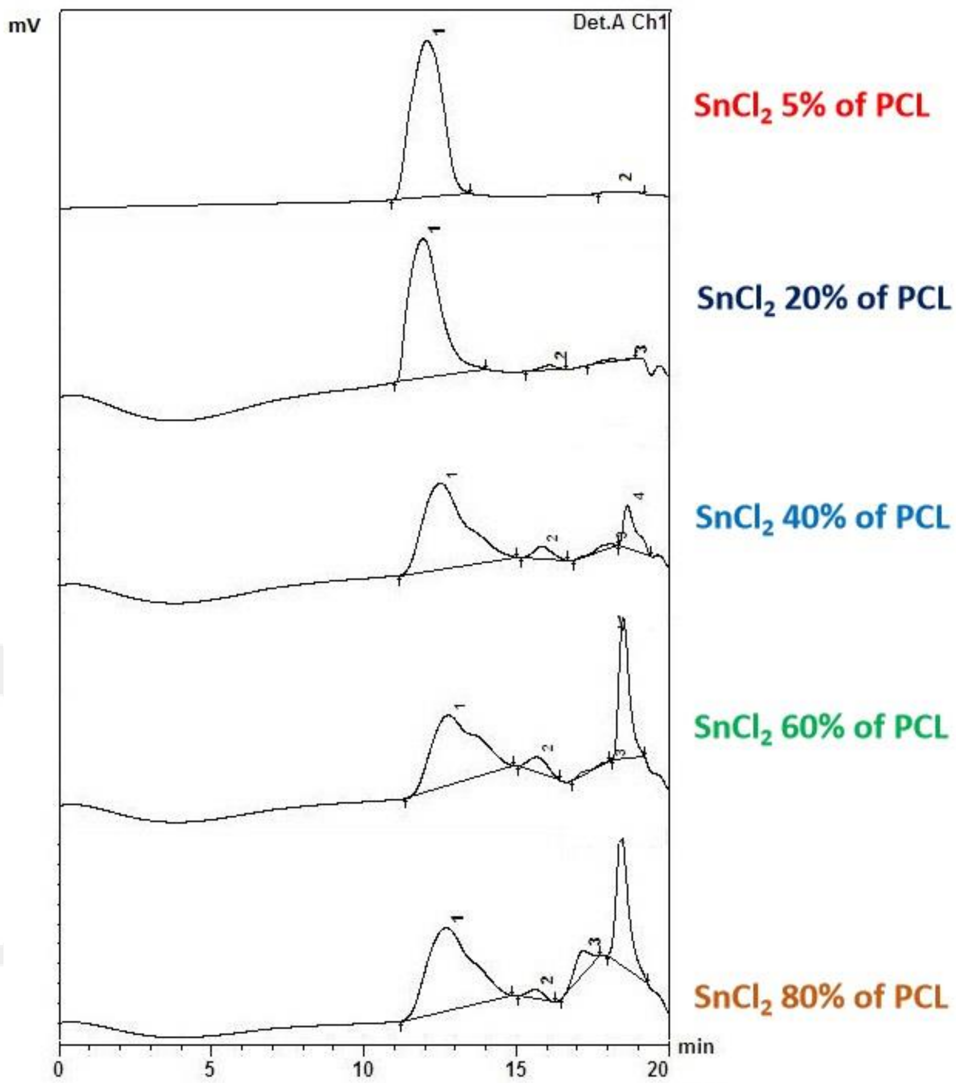

Figure 4.8: GPC results of different percentages of $SnCl_2$ as a degradation catalyst on degradation rate.

Table 4.1 illustrates the molecular weight of degraded PCL and the percentage of degradation values after PCL (80000 Da) pellets were soaked in SBF with the presence of $SnCl_2$ for one week.

Table 4.1: GPC results of PCL pellet degradation by using different amount of $SnCl_2$ catalyst.

	Peak 1 (M_w, Da)	Other Peaks	Degradation (%)
$SnCl_2$ (5%)	～39500	280	1.5
$SnCl_2$ (20%)	～42400	1950,425	3.1
$SnCl_2$ (40%)	23640	2095,540,230	17.4
$SnCl_2$ (60%)	18310	2325,760,290	36.6
$SnCl_2$ (80%)	20900	2500,900,300	～37

However, there is a limit value of tin can be found in materials which are used for human-being, which should be less than 8 ppm. Thus, even if the higher amount of $SnCl_2$ was more effective, the optimum value was chosen as 5% $SnCl_2$ of PCL for health. Each Ti-TiO_2-Ag-PCL_{SnCl2} specimens contained less than 0.5 ppm tin. The degradation percentage of 5% $SnCl_2$ of PCL pellet has increased from 1.5 to 22.5 after 28 days (Table 4.2).

Table 4.2: Degradation (%) of PCL pellet by using 5% $SnCl_2$ as a catalyst after one and four weeks.

	Days	Degradation (%) of PCL
$SnCl_2$ (5%)	7	1.5
$SnCl_2$ (5%)	28	22.5

Since successful results were obtained in the preliminary experiments with pellets, in the next step, PCL solution containing 5% $SnCl_2$ was prepared in chloroform and coated on Ti-TiO_2-Ag samples. After the samples were kept at 37 °C in SBF for 1 and 4 weeks, they were analyzed by GPC. This study was carried out in two steps. In the first step, GPC analysis was performed by taking a sample of the coating on the film and dissolving it in THF. In this step, PCL was seen to be degraded in products with lower M_w (Figure a, Table 4). In the second step, GPC analysis of the SBF solution was performed. First, the solvent of SBF was evaporated and the remainder dissolved in THF. Then these samples were analyzed by GPC. The goal here was to examine the degraded PCL that passed into the SBF.

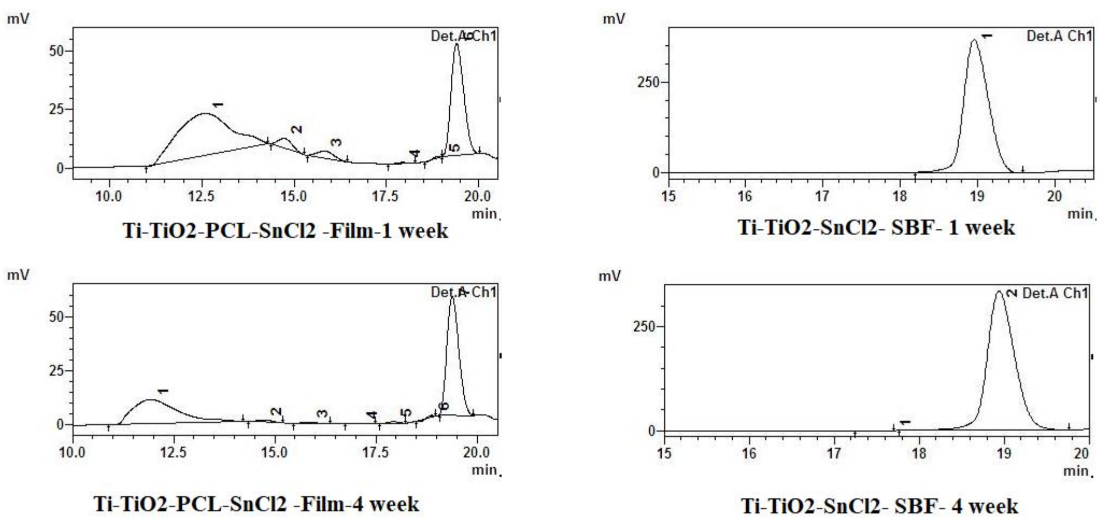

Figure 4.9: GPC analysis of film and residues from 1 to 4 weeks.

Table 4.3: GPC analysis of film and residues from 1 to 4 weeks.

	Peak 1 (M_w, Da)	Other Peaks	Degradation (%)
Film 1 week	～20189	4376, 2163, 508, 231, 122	42.63
Film 4 weeks	～29732	4417, 2124, 968, 511, 228, 126	57.27
SBF 1 week	195	-	-
SBF 4 weeks	198	-	-

As can be seen from the figure and the table, PCL (80000 Da) films degraded to different molecular weights. Some monomer or 6-hydroxy caproic acid and its salts weighing about 195 Da was observed in SBF.

As can be seen from the GPC results given above, $SnCl_2$ showed activity as a catalyst in the degradation of polycaprolactone. Tin(II) chloride compound carries out degradation of polycaprolactone via insertion-coordination mechanism. As seen from Figure 4.10, firstly the tin ion allows coordination of polycaprolactone to tin center through the carbonyl oxygen atom. Secondly, a nucleophilic labile chloride ion attacks the activated carbonyl group, leading to O-acyl scission. In this step, two products are formed which have end groups including chloride and $SnCl^+$ ions. Then, these products hydrolyze with water and hydroxide ion replaces with chloride ion whereas proton ions replace with $SnCl^+$ ion. Finally, degradation products of polycaprolactone are produced which are low M_w PCL (～30000 Da), oligomers (500-4500 Da) and 6-hydroxyl caproic acid as a degradation product of polycaprolactone.

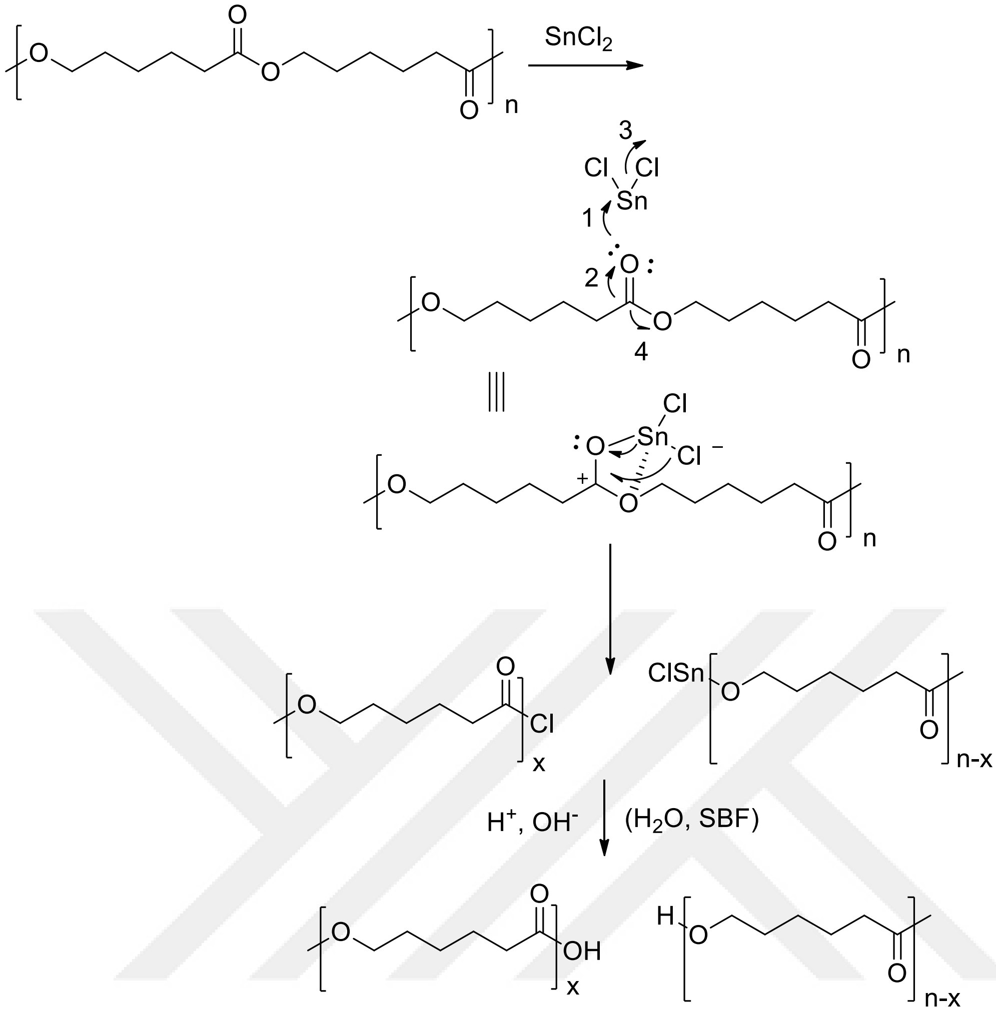

Figure 4.10: Degradation mechanism of PCL with $SnCl_2$.

4.2.3 pH analysis

As it was mentioned before, the initial pH value was 7.4 but pH value change was expected due to degradation of PCL and formation of hydroxyapatite according to BS ISO 23317:2014 - Implants for surgery — In vitro evaluation for apatite-forming ability of implant materials standard. In this case, an increase of the pH was observed. Formation of hydroxyapatite ($Ca_{10} (PO_4)_6 (OH)_2$) increased the pH value because of its basic characteristic. While a significant pH reduction was expected as a result of the degradation of the PCL film, this expectation was not observed. The reasons why the final pH of the solution did not change significantly can be listed as follows: a) the amount of film coated (containing about 20 mg of PCL) is very small compared to the HA formed, b) A very small amount of PCL converts to caproic acid, c) the caproic acid formed is a weak acid.

Table 4.4: The differences in pH values of SBF, Ti-TiO_2-Ag and Ti-TiO_2-Ag-PCL_{SnCl2} after 28 days soaked in SBF.

	Peak 1 (M_w, Da)	Other Peaks	Degradation (%)
Film 1 week	~20189	4376, 2163, 508, 231, 122	42.63
Film 4 weeks	~29732	4417, 2124, 968, 511, 228, 126	57.27
SBF 1 week	195	-	-
SBF 4 weeks	198	-	-

4.2.4 FTIR

FTIR measurements were made separately for the titanium film on the surface and for the SBF. Before FTIR measurements were made, the water in both the film and the SBF was evaporated. The comparison of pure PCL (800000 Da) and PCL on the film surface was made by measuring FTIR. In the FTIR spectrum, the CO band of pure PCL appears at 1721 cm^{-1}, while the appearance of the CO band of the film 1629 cm^{-1} indicates that PCL is degraded and interacts with other ions (Ca^{2+}, Na^{+}) in SBF and $SnCl_2$. As can be seen from Figure 4.11 and Table 4.5, other FTIR peaks of degradation products of PCL are in agreement with the peaks of pure PCL.

While PCL (80000 Da) does not have an OH peak, the appearance of the OH peak at 3414 cm^{-1} in the film indicates that PCL is hydrolyzed.

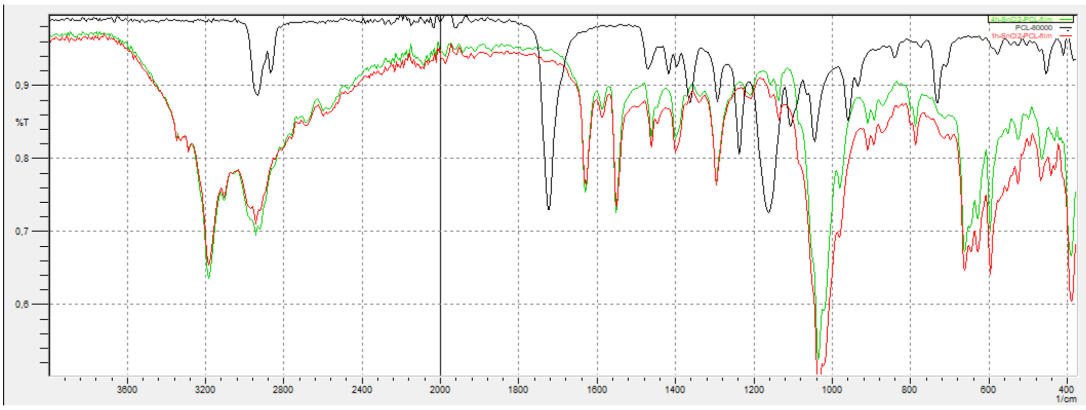

Figure 4.11: FTIR spectra of a) PCL80000 Da (black line), b) film after 1 week in SBF (red line) and c) film after 4 weeks in SBF (green line).

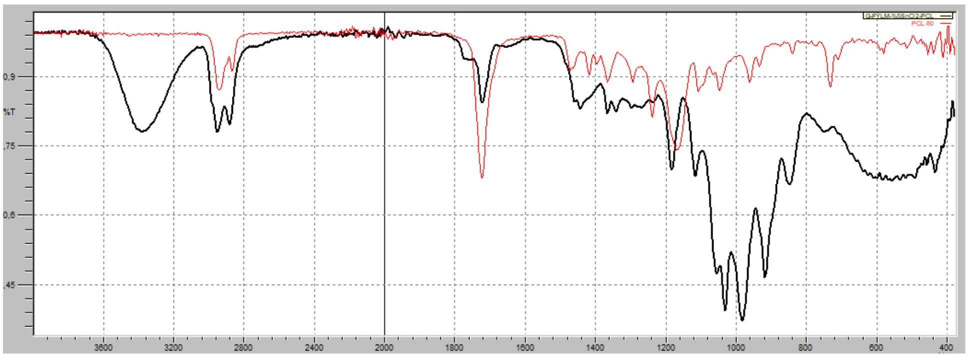

Figure 4.12: FTIR spectra of PCL 80000 Da (red line) and dried SBF including degraded PCL (black line, after 4 weeks).

In addition to the GPC measurements, FTIR measurements were made to prove the presence of degraded PCL in SBF. Since the amount of degraded PCL is low, the solvent of the SBF solution was evaporated first. Then degraded PCL was extracted with THF and finally dried and FTIR analysis was performed. As can be seen from Figure 4.12, it belongs to the peak carboxyl or carboxylate group that appears at 1757.95 cm^{-1}, which indicates that PCL is degraded to 6-hydroxy caproic acid or 6-hydroxy caproate. The OH peak at 3378.83 cm^{-1} belongs to both 6-hydroxy caproic acid and formation of amorphous biomimetic HA.

When FTIR analysis of the solid part (HA part) insoluble in THF is done, the characteristic peaks of CO_3^{2-} and PO_4^{3-} groups in hydroxyapatite (HA) were observed. The phosphate peaks at 530-564 for $\nu_{bending}$ (O-P-O) and 1041 cm^{-1} for ν_{as} (P-O); carbonate peak at 1494 cm^{-1} for $\nu_{streching}$ (C-O) and 1454 cm^{-1} for $\nu_{bending}$ (C-O) showed the formation of apatite ($Ca_5(PO_4)_3(OH, CO_3^{2-})$).

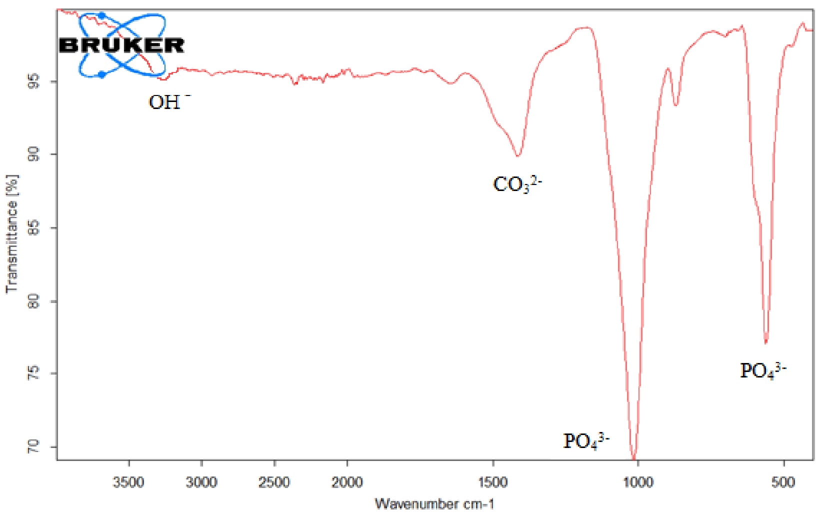

Figure 4.13: FTIR spectrum of part (HA part) insoluble in THF.

At the end of the measurements, peaks of the analyzed samples were compared to the characteristic peaks of hydroxyapatite and it was seen that the peaks of the samples matched the characteristic ones (Figure 4.11) (Table (4.5 [86])). In other words, these characteristic FTIR peaks are in agreement with the literature data of hydoxyapatite.

Table 4.5: Characteristic wavenumber of PCL FTIR Spectra [86].

PCL FTIR Spectra	Wavenumber cm^{-1}
Symmetric COC stretching v_s (COC)	~1170
OC-O stretching v(OC-O)	~1190
Asymmetric COC stretching	~1240
C-O and C-O and C-C stretching in the crystalline phase	~1293
Carbonyl stretching v_{as}(C=O)	~1727
Symmetric CH_2 stretching $v_s(CH_2)$	~2865
Asymmetric CH_2 stretching $v_{as}(CH_2)$	~2943

Table 4.6: Characteristic wavenumber of HA FTIR Spectra [86].

HA FTIR Spectra	Wavenumber cm^{-1}
OH stretching	~3568
CO_3^{2-}	~1494 (stretching), 1454,1436, 868 (bending)
PO_4^{3-}	1190-900 (Asymmetric stretching), 635-530 (Asymmetric bending vibration)

4.2.5 AAS

After PCL degradation, silver release was measured by atomic absoption spectroscopy analysis. Firstly, Ti-TiO_2-Ag sample (blue line in graph) that was not coated with PCL was soaked into SBF solution. Silver release was measured every day. The maximum amount of silver release was measured on the first day and these values decreased day by day. Definite results could not be obtained on the 6th and especially on the 7th day since the values were below the reading limit of the AAS device. After that, the PCL coated samples (orange line in graph) were placed in the SBF solution and their characterization was performed at the end of the 1st, 2nd, 3rd and 4th weeks, keeping all parameters the same.

The release of silver was delayed by the PCL coating including $SnCl_2$, which was the motivation of this study. With the degradation of the PCL coating, silver release took place. Contrary to the first case, there was an increase in the amount of silver release every week. This can be explained by the increasing amount of degradation of the polymer as it stays in the SBF solution.

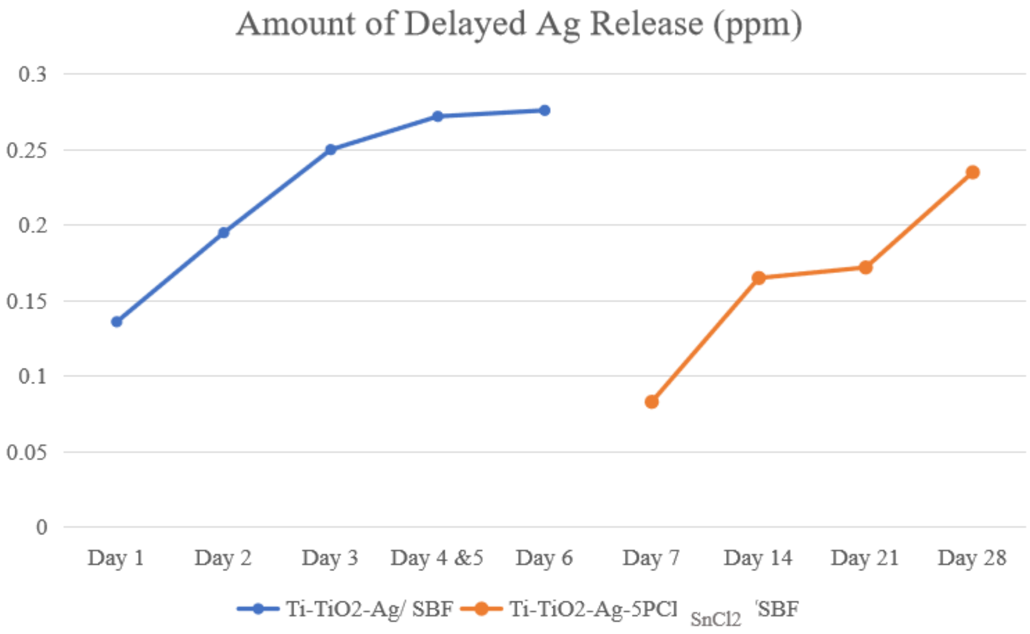

Figure 4.14: Amount of Ag release of Ti-TiO_2-Ag/ SBF and Ti-TiO_2-Ag-5PCL/SBF by AAS analysis.

As can be seen from Table 4.7, the amount of released silver at the end of the 1st week and at the end of the 4th week was 0.083 ppm and 0.235 ppm, respectively. The silver release of the PCL coated samples is 85% of the silver release of the non-PCL coated sample after 28 days.

Table 4.7: Comparison of total amount of silver release between uncoated and coated PCL titanium samples from first to fourth week.

Chemicals	Formula	Solubility
Ti-TiO_2-Ag/ SBF	0.276	7
Ti-TiO_2-Ag-PCL_{SnCl2}/ SBF	0.083	7
Ti-TiO_2-Ag-PCL_{SnCl2}/ SBF	0.165	14
Ti-TiO_2-Ag-PCL_{SnCl2}/ SBF	0.172	21
Ti-TiO_2-Ag-PCL_{SnCl2}/ SBF	0.235	28

5. CONCLUSION

This study covers the coating of antibacterial silver doped titanium with biodegradable PCL in dental implants and the gradual release of silver by degradation of PCL. The characterizations made showed the efficiency of each experimental stage. Optical microscope results showed that the MAO process increased the adhesion between Ti and the coating. In addition, it was observed that the amount of amorphous biomimetic HA seen on the sample surface gradually increased as soaked in the SBF.

The regular, spherical porous structure desired for controlled drug release was achieved by selecting the appropriate MAO parameters. Then, silver was doped on Ti with the MAO process to show antibacterial properties and the new dendritic structures formed were observed with SEM. Chemical analysis of these structures was done with EDS and XRD. $CaTiO_3$, Ag_2O, and TiO_2 in rutile and anatase were found.

Considering the time targeted in this thesis, $SnCl_2$ was used for the first time as a degradation catalyst to find a solution to the slow degradation disadvantage of PCL. According to the GPC results made in the preliminary experiment, it was observed that the catalyst activity increased with the increase in the amount of $SnCl_2$. At this stage, 5% $SnCl_2$ was chosen as the degradation catalyst with minimal toxicity and sufficient catalyst activity in the desired time.

After preparing the appropriate coating solution, it was coated on Ti-TiO_2 and immersed in SBF for 1-4 weeks and two different GPC analysis of these samples were performed. Initially, the films were dissolved in THF and GPC analysis of these solutions showed that the film degraded 42.63% in the first week and 57.27% at the end of the fourth week. Secondly, when the GPC results of the samples taken from the SBF solution were examined, a peak around 195 Da was observed both in the first week and in the fourth week. It was determined that this peak belonged to 6-hydroxy caproic acid or its salt formed as a result of PCL degradation. It was observed that the 1721 cm^{-1} and 1757 cm^{-1} peaks seen in the FTIR analysis also supported this result. When the FTIR peaks of PCL coated on the sample and Pure

PCL were compared, it was seen that the coated PCL interacted with the ions in SBF and $SnCl_2$ and therefore the peaks were shifted. Moreover, the OH peak in the FTIR spectrum of the coated PCL was also seen to support the degradation of the PCL. HA was observed in FTIR analysis taken from the solid part. In pH measurements, it was determined that the increase in pH was caused by the HA formed.

Finally, two different setups were prepared to compare the change in silver release with PCL coating. It was observed that the silver release in the SBF of the non-PCL-coated sample was maximum on the first day and then decreased day by day. On the contrary, PCL coated samples started release from the first week and reached the highest value in the fourth week. This demonstrated that the PCL was gradually degraded, and the desired silver release was achieved within the targeted time. As a result of this thesis, the silver release can be extended to the desired time by adjusting the catalyst amount.

REFERENCES

[1] **Ramos, B. G. Z.** (2011). Biopolymers employed in drug delivery. Biopolymers: Biomédical and Environmental Applications, 559.

[2] **Bose, S., Vu, A. A., Emshadi, K., & Bandyopadhyay, A. (2018**). Effects of polycaprolactone on alendronate drug release from Mg-doped hydroxyapatite coating on titanium. *Materials Science and Engineering: C, 88,* 166-171.

[3] **Lan, S. F. Kehinde, T., Zhang, X., Khajotia, S., Schmidtke, D. W., & Starly, B. (2013).** Controlled release of metronidazole from composite poly-ε-caprolactone/alginate (PCL/alginate) rings for dental implants. *Dental materials*, *29*(6), 656-665.

[4] **Smith, A. M., Moxon, S., & Morris, G. A. (2016).** Biopolymers as wound healing materials. In *Wound Healing Biomaterials* (pp. 261-287). Woodhead Publishing.

[5] **França, D. C., Bezerra, E. B., Morais, D. D. D. S., Araújo, E. M., & Wellen, R. M. R. (2016).** Hydrolytic and thermal degradation of PCL and PCL/bentonite compounds. *Materials Research*, *19*(3), 618-627.

[6] **Rezaei, A., & Mohammadi, M. R. (2013).** In vitro study of hydroxyapatite/polycaprolactone (HA/PCL) nanocomposite synthesized by an in situ sol–gel process. *Materials Science and Engineering: C*, *33*(1), 390-396.

[7] **Brannigan, R. P., & Dove, A. P. (2017).** Synthesis, properties and biomedical applications of hydrolytically degradable materials based on aliphatic polyesters and polycarbonates. *Biomaterials science*, *5*(1), 9-21.

[8] **Ghorbani, F. M., Kaffashi, B., Shokrollahi, P., Seyedjafari, E., & Ardeshirylajimi, A. (2015).** PCL/chitosan/Zn-doped nHA electrospun nanocomposite scaffold promotes adipose derived stem cells adhesion and proliferation. *Carbohydrate polymers*, *118*, 133-142.

[9] **Laycock, B., Nikolić, M., Colwell, J. M., Gauthier, E., Halley, P., Bottle, S., & George, G. (2017).** Lifetime prediction of biodegradable polymers. *Progress in Polymer Science*, *71*, 144-189.

[10] **Dash, T. K., & Konkimalla, V. B. (2012).** Polymeric modification and its implication in drug delivery: poly-ε-caprolactone (PCL) as a model polymer. *Molecular pharmaceutics*, *9*(9), 2365-2379

[11] **Yazdimamaghani, M., Razavi, M., Vashaee, D., & Tayebi, L. (2014).** Development and degradation behavior of magnesium scaffolds coated with polycaprolactone for bone tissue engineering. *Materials Letters*, *132*, 106-110.

[12] **McCracken, M. (1999).** Dental implant materials: commercially pure titanium and titanium alloys. *Journal of prosthodontics*, *8*(1), 40-43.

[13] **Oldani, C., & Dominguez, A.** (2012). Titanium as a Biomaterial for Implants. *Recent advances in arthroplasty*, *218*, 149-162.

[14] **Niinomi, M., & Nakai, M.** (2011). Titanium-based biomaterials for preventing stress shielding between implant devices and bone. *International journal of biomaterials*, *2011*.

[15] **He, X., Zhang, X., Wang, X., & Qin, L.** (2017). Review of antibacterial activity of titanium-based implants' surfaces fabricated by micro-arc oxidation. *Coatings*, *7*(3), 45

[16] **Jaiswal, S., McHale, P., & Duffy, B.** (2012). Preparation and rapid analysis of antibacterial silver, copper and zinc doped sol–gel surfaces. *Colloids and Surfaces B: Biointerfaces*, *94*, 170-176.

[17] **Bruschi, M. L.** (2015). *Strategies to modify the drug release from pharmaceutical systems*. Woodhead Publishing.

[18] **Bhowmik, D., Gopinath, H., Kumar, B. P., Duraivel, S., & Kumar, K. S.** (2012). Controlled release drug delivery systems. *The Pharma Innovation*, *1*(10, Part A), 24.

[19] **Bajpai, A. K., Shukla, S. K., Bhanu, S., & Kankane, S.** (2008). Responsive polymers in controlled drug delivery. *Progress in Polymer Science*, *33*(11), 1088-1118.

[20] **Lin, C. C., & Metters, A. T.** (2006). Hydrogels in controlled release formulations: network design and mathematical modeling. *Advanced drug delivery reviews*, *58*(12-13), 1379-1408.

[21] **Ryu, H. S., Bae, I. H., Lee, K. G., Hwang, H. S., Lee, K. H., Koh, J. T., & Cho, J. H.** (2012). Antibacterial effect of silver-platinum coating for orthodontic appliances. *The Angle Orthodontist*, *82*(1), 151-157.

[22] **Malachová, K., Praus, P., Rybková, Z., & Kozák, O.** (2011). Antibacterial and antifungal activities of silver, copper and zinc montmorillonites. *Applied Clay Science*, *53*(4), 642-645.

[23] **Nishanthi, R., Malathi, S., & Palani, P.** (2019). Green synthesis and characterization of bioinspired silver, gold and platinum nanoparticles and evaluation of their synergistic antibacterial activity after combining with different classes of antibiotics. *Materials Science and Engineering: C*, *96*, 693-707.

[24] **Marshall, B. J., Armstrong, J. A., Francis, G. J., Nokes, N. T., & Wee, S. H.** (1987). Antibacterial action of bismuth in relation to Campylobacter pyloridis colonization and gastritis. *Digestion*, *37*(Suppl. 2), 16-30.

[25] **Yun'an Qing, L. C., Li, R., Liu, G., Zhang, Y., Tang, X., Wang, J., ... & Qin, Y.** (2018). Potential antibacterial mechanism of silver nanoparticles and the optimization of orthopedic implants by advanced modification technologies. International journal of nanomedicine, 13, 3311.

[26] **Kaur, A., & Kumar, R.** (2019). Enhanced bactericidal efficacy of polymer stabilized silver nanoparticles in conjugation with different classes of antibiotics. *RSC advances*, *9*(2), 1095-1105.

[27] **Zhang, P., Zhang, Z., & Li, W.** (2013). Antibacterial coating incorporating silver nanoparticles by microarc oxidation and ion implantation. *Journal of Nanomaterials*, *2013*.

[28] **Wang, X., Hou, X., Luan, W., Li, D., & Yao, K.** (2012). The antibacterial and hydrophilic properties of silver-doped TiO2 thin films using sol–gel method. *Applied surface science*, *258*(20), 8241-8246.

[29] **Wakshlak, R. B. K., Pedahzur, R., & Avnir, D.** (2015). Antibacterial activity of silver-killed bacteria: the" zombies" effect. *Scientific reports*, *5*, 9555.

[30] **Lansdown, A. B.** (2002). Silver I: its antibacterial properties and mechanism of action. *Journal of wound care*, *11*(4), 125-130.

[31] **Jung, W. K., Koo, H. C., Kim, K. W., Shin, S., Kim, S. H., & Park, Y. H.** (2008). Antibacterial activity and mechanism of action of the silver ion in Staphylococcus aureus and Escherichia coli. *Appl. Environ. Microbiol.*, *74*(7), 2171-2178.

[32] **Fayaz, A. M., Balaji, K., Girilal, M., Yadav, R., Kalaichelvan, P. T., & Venketesan, R. (2010).** Biogenic synthesis of silver nanoparticles and their synergistic effect with antibiotics: a study against gram-positive and gram-negative bacteria. *Nanomedicine: Nanotechnology, Biology and Medicine*, *6*(1), 103-109.

[33] **Romero-Urbina, D. G., Lara, H. H., Velázquez-Salazar, J. J., Arellano-Jiménez, M. J., Larios, E., Srinivasan, A., ... & Yacamán, M. J.** (2015). Ultrastructural changes in methicillin-resistant Staphylococcus aureus induced by positively charged silver nanoparticles. *Beilstein journal of nanotechnology*, *6*(1), 2396-2405.

[34] **Râpă, M., Stoica, P., Tănase, E. E., Grosu, E., & Vlad, G.** (2013). Preparation of medical devices with antimicrobial properties. *Journal Of Optoelectronics And Advanced Materials*, *15*(7-8), 807-816.

[35] **Lackner, M.** (2000). Bioplastics. *Kirk-Othmer Encyclopedia of Chemical Technology*, 1-41.

[36] **Tokiwa, Y., Calabia, B. P., Ugwu, C. U., & Aiba, S.** (2009). Biodegradability of plastics. *International journal of molecular sciences*, *10*(9), 3722-3742.

[37] **Albertsson, A. C., & Srivastava, R. K.** (2008). Recent developments in enzyme-catalyzed ring-opening polymerization. *Advanced drug delivery reviews*, *60*(9), 1077-1093.

[38] **Azevedo, H. S., & Reis, R. L.** (2005). Understanding the enzymatic degradation of biodegradable polymers and strategies to control their degradation rate. *Biodegradable systems in tissue engineering and regenerative medicine*, 177-201.

[39] **Darwis, D., Mitomo, H., Enjoji, T., Yoshii, F., & Makuuchi, K.** (1998). Enzymatic degradation of radiation crosslinked poly (ε–caprolactone). *Polymer Degradation and Stability, 62*(2), 259-265.

[40] **Holland, S. J., Jolly, A. M., Yasin, M., & Tighe, B. J.** (1987). Polymers for biodegradable medical devices: II. Hydroxybutyrate-hydroxyvalerate copolymers: Hydrolytic degradation studies. *Biomaterials*, *8*(4), 289-295.

[41] **Dziadek, M., Pawlik, J., Menaszek, E., Stodolak-Zych, E., & Cholewa-Kowalska, K.** (2015). Effect of the preparation methods on architecture, crystallinity, hydrolytic degradation, bioactivity, and biocompatibility of PCL/bioglass composite scaffolds. *Journal of Biomedical Materials Research Part B: Applied Biomaterials*, *103*(8), 1580-1593.

[42] **van Bochove, B., & Grijpma, D. W.** (2019). Photo-crosslinked synthetic biodegradable polymer networks for biomedical applications. *Journal of Biomaterials Science, Polymer Edition*, *30*(2), 77-106.

[43] **Rabin, C. R., & Siegel, S. J.** (2012). Delivery systems and dosing for antipsychotics. In *Current Antipsychotics* (pp. 267-298). Springer, Berlin, Heidelberg.

[44] **Vieira, A. C., Guedes, R. M., & Tita, V.** (2013). Considerations for the design of polymeric biodegradable products. *Journal of Polymer Engineering, 33*(4), 293-302.

[45] **Davison, N. L., Barrère-de Groot, F., & Grijpma, D. W.** (2014). Degradation of biomaterials. In *Tissue Engineering* (pp. 177-215). Academic Press.

[46] **Kumar, S., & Thakur, K. S.** (2017). Bioplastics-classification, production and their potential food applications. *Journal of Hill Agriculture*, *8*(2), 118-129.]

[47] **Kayan, A.** Recent Studies on Single Site Metal Alkoxide Complexes as Catalysts for Ring Opening Polymerization of Cyclic Compounds. *Catalysis Surveys from Asia*, 1-17.

[48] **Leja, K., & Lewandowicz, G.** (2010). Polymer Biodegradation and Biodegradable Polymers-a Review. Polish Journal of Environmental Studies, 19(2)

[49] **Malikmammadov, E., Tanir, T. E., Kiziltay, A., Hasirci, V., & Hasirci, N.** (2018). PCL and PCL-based materials in biomedical applications. *Journal of Biomaterials science, Polymer edition*, *29*(7-9), 863-893.

[50] **Miller-Chou, B. A., & Koenig, J. L.** (2003). A review of polymer dissolution. *Progress in Polymer Science*, *28*(8), 1223-1270.

[51] **Speight, J. G.** (2011). Chapter 14-Monomers, Polymers, and Plastics. *Handbook of Industrial Hydrocarbon Processes*, 499-537.

[52] **Ashter, S. A.** (2016). *Introduction to bioplastics engineering*. William Andrew.

[53] **Jasso-Gastinel, C. F., Soltero-Martínez, J. F. A., & Mendizábal, E.** (2017). Introduction: modifiable characteristics and applications. In *Modification of Polymer Properties* (pp. 1-21). William Andrew Publishing.

[54] **Sun, H., Mei, L., Song, C., Cui, X., & Wang, P.** (2006). The in vivo degradation, absorption and excretion of PCL-based implant. *Biomaterials*, *27*(9), 1735-1740.

[55] **Heimowska, A., Morawska, M., & Bocho-Janiszewska, A.** (2017). Biodegradation of poly (ε-caprolactone) in natural water environments. *Polish Journal of Chemical Technology*, *19*(1), 120-126.

[56] **Sánchez-González, S., Diban, N., & Urtiaga, A.** (2018). Hydrolytic degradation and mechanical stability of poly (ε-Caprolactone)/reduced graphene oxide membranes as scaffolds for in vitro neural tissue regeneration. *Membranes*, *8*(1), 12.

[57] **Scaffaro, R., Maio, A., Sutera, F., Gulino, E. F., & Morreale, M.** (2019). Degradation and recycling of films based on biodegradable polymers: A short review. *Polymers*, *11*(4), 651

[58] **Gu, X. N., Li, N., Zhou, W. R., Zheng, Y. F., Zhao, X., Cai, Q. Z., & Ruan, L.** (2011). Corrosion resistance and surface biocompatibility of a microarc oxidation coating on a Mg–Ca alloy. *Acta Biomaterialia*, *7*(4), 1880-1889.

[59] **Li, Q**. (2013). Sol-gel coatings to improve the corrosion resistance of magnesium (Mg) alloys. In *Corrosion Prevention of Magnesium Alloys* (pp. 469-485). Woodhead Publishing.

[60] **Aziz, F., & Ismail, A. F.** (2015). Spray coating methods for polymer solar cells fabrication: A review. *Materials Science in Semiconductor Processing*, *39*, 416-425

[61] **Cremer, M. D., Hart, S. D., Henry, D., O'malley, S. M., & Schneider, V. M.** (2014). *U.S. Patent Application No. 14/095,217*.

[62] **Busuioc, C., Jinga, S. I., & Andronescu, E.** (2012). Barium magnesium tantalate thin films obtained by sol-gel processing. Revista Romana de Materiale, 42(3), 299-305.

[63] **Raut, H. K., Ganesh, V. A., Nair, A. S., & Ramakrishna, S.** (2011). Anti-reflective coatings: A critical, in-depth review. *Energy & Environmental Science*, *4*(10), 3779-3804.

[64] **Karthikeyan, J.** (2007). The advantages and disadvantages of the cold spray coating process. In *The cold spray materials deposition process* (pp. 62-71). Woodhead Publishing.

[65] **Sahoo, S. K., Manoharan, B., & Sivakumar, N.** (2018). Introduction: Why Perovskite and Perovskite Solar Cells?. In *Perovskite Photovoltaics* (pp. 1-24). Academic Press.

[66] **Neacşu, I. A., Nicoară, A. I., Vasile, O. R., & Vasile, B. Ş.** (2016). Inorganic micro-and nanostructured implants for tissue engineering. In *Nanobiomaterials in Hard Tissue Engineering* (pp. 271-295). William Andrew Publishing.

[67] **Ji, G., & Zhao, M.** (2017). Membrane separation technology in carbon capture. *Recent Advances in Carbon Capture and Storage; Yun, Y., Ed*, 59-90

[68] **Oliveira, P. W., Mennig, M., Aegerter, M. A., & Schmidt, H.** (2004). Interference coatings. In *Sol-Gel Technologies for Glass Producers and Users* (pp. 195-206). Springer, Boston, MA.

[69] **Rio, E., & Boulogne, F.** (2017). Withdrawing a solid from a bath: How much liquid is coated?. *Advances in colloid and interface science, 247*, 100-114.

[70] **Sanchez-Herencia, A. J.** (2007). Water based colloidal processing of ceramic laminates. In *Key Engineering Materials* (Vol. 333, pp. 39-48). Trans Tech Publications Ltd.

[71] **Hume, P. S., Bowman, C. N., & Anseth, K. S.** (2011). Functionalized PEG hydrogels through reactive dip-coating for the formation of immunoactive barriers. *Biomaterials*, *32*(26), 6204-6212.

[72] **Landrock, A. H., & Ebnesajjad, S.** (2008). *Adhesives technology handbook*. William Andrew.

[73] **Wypych, G.** (2004). Plasticizers in Various Processing Methods. *Handbook of Plasticizers*, 471.

[74] **Wang, Y., Yu, H., Chen, C., & Zhao, Z**. (2015). Review of the biocompatibility of micro-arc oxidation coated titanium alloys. *Materials & Design*, *85*, 640-652.

[75] **Kim, Y. K., Lee, K. B., Kim, S. Y., Jang, Y. S., Kim, J. H., & Lee, M. H.** (2018). Improvement of osteogenesis by a uniform PCL coating on a magnesium screw for biodegradable applications. *Scientific reports*, *8*(1), 1-11.

[76] **Li, L. H., Narayanan, T. S., Kim, Y. K., Kong, Y. M., Park, I. S., Bae, T. S., & Lee, M. H.** (2014). Deposition of microarc oxidation–polycaprolactone duplex coating to improve the corrosion resistance of magnesium for biodegradable implants. *Thin Solid Films, 562*, 561-567.

[77] **Yao, X., Zhang, X., Wu, H., Tian, L., Ma, Y., & Tang, B.** (2014). Microstructure and antibacterial properties of Cu-doped TiO2 coating on titanium by micro-arc oxidation. *Applied Surface Science*, *292*, 944-947.

[78] **Brunette, D. M., Tengvall, P., Textor, M., & Thomsen, P.** (Eds.). (2012). *Titanium in medicine: material science, surface science, engineering, biological responses and medical applications*. Springer Science & Business Media.

[79] **Cui, C., Hu, B., Zhao, L., & Liu, S.** (2011). Titanium alloy production technology, market prospects and industry development. *Materials & Design*, *32*(3), 1684-1691.

[80] **Yazdani, J., Ahmadian, E., Sharifi, S., Shahi, S., & Dizaj, S. M.** (2018). A short view on nanohydroxyapatite as coating of dental implants. *Biomedicine & Pharmacotherapy, 105*, 553-557.

[81] **Acero, J., Calderon, J., Salmeron, J. I., Verdaguer, J. J., Concejo, C., & Somacarrera, M. L.** (1999). The behaviour of titanium as a biomaterial: microscopy study of plates and surrounding tissues in facial osteosynthesis. *Journal of Cranio-Maxillofacial Surgery*, *27*(2), 117-123.

[82] **Le Guéhennec, L., Soueidan, A., Layrolle, P., & Amouriq, Y.** (2007). Surface treatments of titanium dental implants for rapid osseointegration. *Dental materials*, 23(7), 844-854.

[83] **Bowden, F. P., Bowden, F. P., & Tabor, D.** (2001). *The friction and lubrication of solids* (Vol. 1). Oxford university press.

[84] **Packham, D. E.** (2003). Surface energy, surface topography and adhesion. *International journal of adhesion and adhesives*, *23*(6), 437-448.

[85] **Yeo, I. S., Kim, H. Y., Lim, K. S., & Han, J. S.** (2012). Implant surface factors and bacterial adhesion: a review of the literature. *The International journal of artificial organs*, *35*(10), 762-772.

[86] **Garskaite, E., Gross, K. A., Yang, S. W., Yang, T. C. K., Yang, J. C., & Kareiva, A.** (2014). Effect of processing conditions on the crystallinity and structure of carbonated calcium hydroxyapatite (CHAp). *CrystEngComm*, *16*(19), 3950-3959.

APPENDICES

APPENDIX A: EDS Result

APPENDIX A:

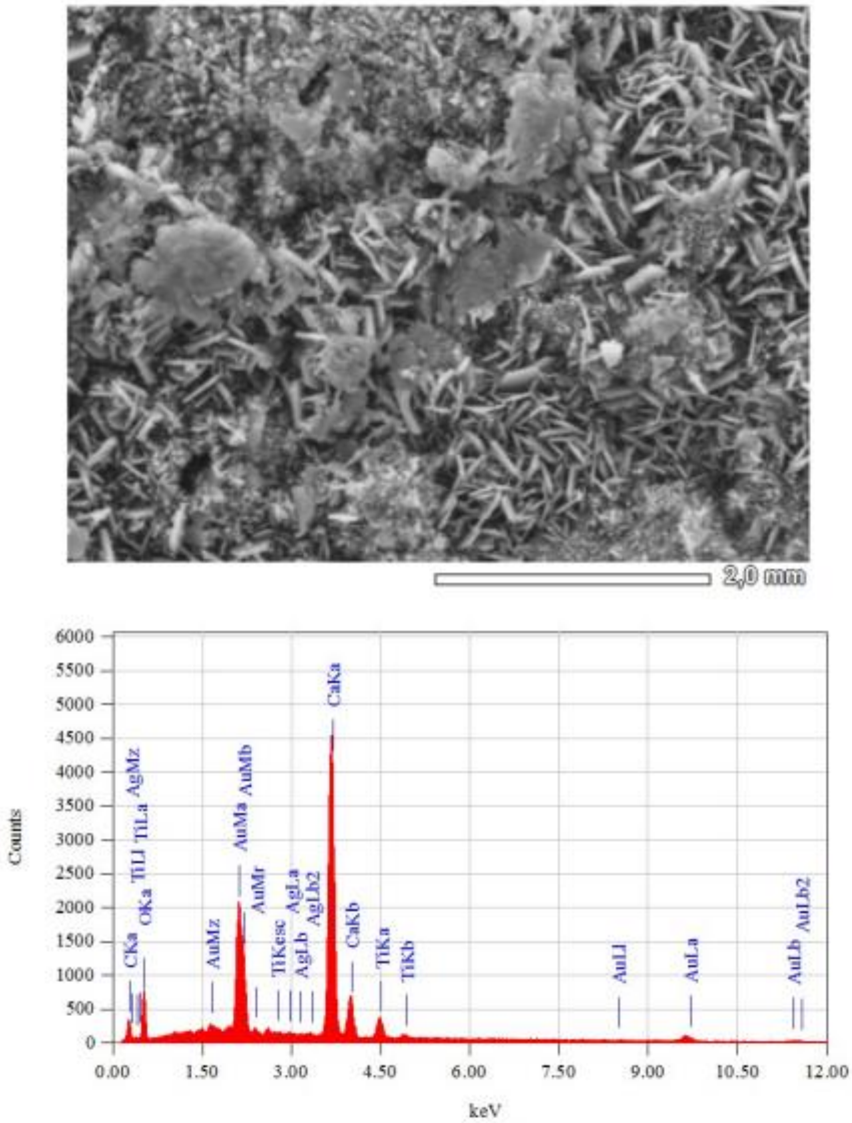

Element	Mass %
O	52.943
Ca	42.06
Ti	4.480
Ag	0.533

Figure A.1: EDS results of previous experiment

CURRICULUM VITAE

Name Surname **:** Gizem Özge KAYAN

EDUCATION

- **M.Sc. :** 2021, Istanbul Technical University, Chemical and Metallurgical Engineering Faculty , Metallurgical and Materials Engineering Department

- **B.Sc. :** 2018, Istanbul Technical University, Chemical and Metallurgical Engineering Faculty, Metallurgical and Materials Engineering Department